PAPER G

CROSS-WELL REFLECTION VELOCITY ANALYSIS

Nicholas Smalley

ABSTRACT

A method of cross-well reflection velocity analysis is introduced in this paper. It uses previously derived cross-well reflection moveout equations (Smalley, 1992). These moveout equations are based upon a previously derived cross-well CLP (common lateral point) stacking coordinate system (Smalley, 1992). The method showed in this paper has a similar objective to the surface seismic velocity analysis procedure. We are attempting to find velocities from the cross-well reflections that will give us an accurate depth conversion and can align the reflection data so that the stack will be optimized. The cross-well gather analogous to the surface seismic CMP gather (CLP - VLMO gather) is used to align reflection data so that the stack will be optimized. The horizontally corrected common lateral point gather (CLP - HNMO) is used to help find the correct reflector depth. The theory is derived for the constant velocity case and then is extended to the variable velocity case. Synthetics are shown for both of these cases. Real data gathers and stacks are shown using the cross-well reflection velocity analysis and are compared to stacks using tomogram velocities. The stacks from using the cross-well reflection analysis show a clear improvement from constant velocity tomogram stacks.

INTRODUCTION

Cross-well reflection imaging theory is still early in its development. Recently two new methods of cross-well reflection imaging have been proposed. The first of these was based on the XSP - CDP transform (Lazaratos, 1991, 1992) which is a modified version of the VSP - CDP transform. The results from this work are quite promising, but are dependent on tomogram and well log velocities. Additionally, the amount of work and residual statics or moveout corrections due to the inaccuracies of tomogram and well log velocities make the

work to obtain coherent reflections by this method cumbersome. Because tomograms may not be reliable, especially in the case of wide well separation, it is important to develop a method for obtaining velocities which will align reflections and give us an accurate depth conversion using the reflection data. By doing this we can obtain stacking velocities or slownesses that stack the reflections coherently and gives us a way to account for lateral velocity variation. Recently a new cross-well reflection imaging algorithm was proposed (Smalley, 1992). This algorithm develops a parallel between cross-well and surface seismic reflection CDP stacking and imaging. By doing this it enables us to combine the well-known stacking and imaging techniques of surface seismic with the intrinsically high resolution data of cross-well. One of the key benefits is having traveltime moveout equations for cross-well reflection velocity analysis. Velocity analysis is essential in surface seismic reflection imaging to obtain the ideal stacking velocities for the NMO correction. It is done by considering CMP gathers and finding time - velocity pairs that give the maximum semblance as a function of time. The NMO equation in surface seismic is

$$t^2 = t_o^2 + \frac{f^2}{v^2}, \tag{1}$$

where f is the offset between the source and geophone, and v is the actual earth velocity in a constant velocity medium, and is the stacking velocity (approximated by the RMS velocity in a v(z) medium). As will be seen, the moveout equations for cross-well will be used in doing cross-well reflection velocity analysis. The situation for cross-well will be more complicated than surface seismic velocity analysis. For a reflection at a given depth, the sources and geophones used to stack this reflection transverse different layers, unlike surface seismic (Figure 1). Therefore a single stacking velocity cannot be assigned to an individual reflection except in a constant velocity case.

CROSS-WELL REFLECTION VELOCITY ANALYSIS AND DEPTH CONVERSION - CONSTANT SLOWNESS

The cross-well gather analogous to the NMO corrected CMP gather is the HNMO and VLMO corrected CLP gather (CLP - VLMO) (Figure 2) (Smalley, 1992). The final stack is carried out over the radial distance coordinate (analogous to the surface seismic coordinate of offset). Therefore we want to attempt to maximize the semblance at the assumed reflector depth, by finding the appropriate HNMO and VLMO velocities.

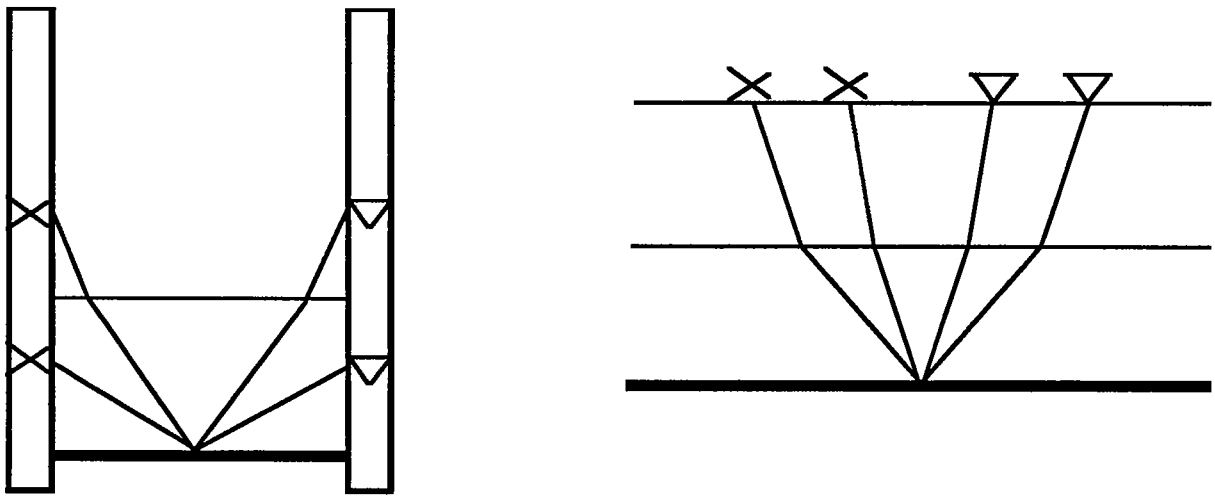

Figure 1. Stacking in cross-well reflection imaging versus stacking in surface seismic. The problem is more difficult in cross-well due to the raypath coverage of the cross-well common lateral point gathers.

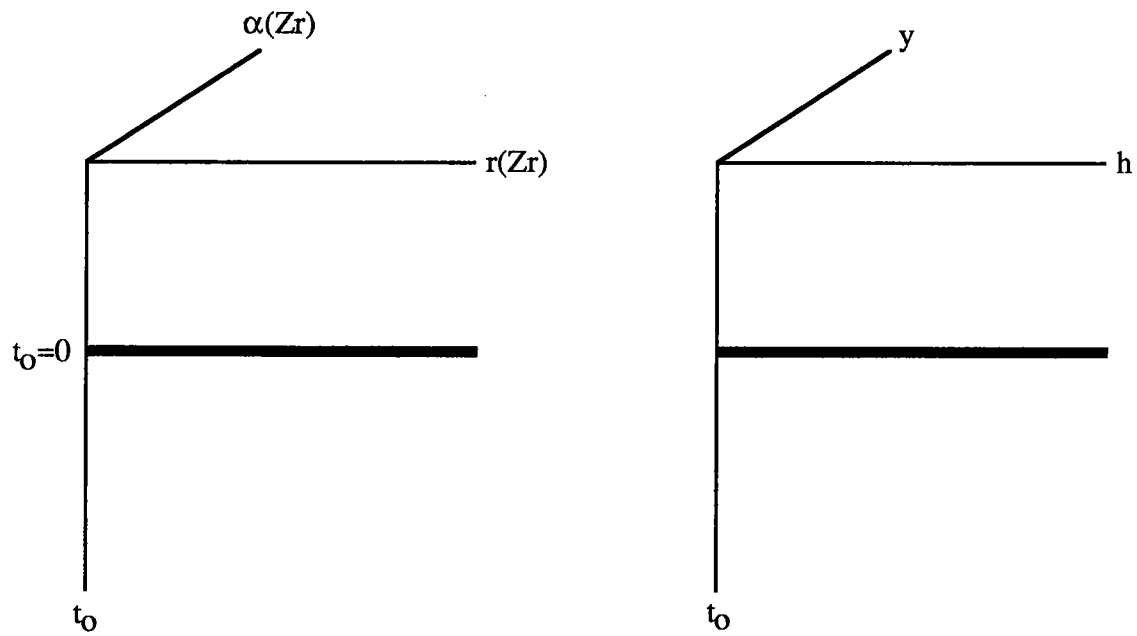

Figure 2. CLP - VLMO gather in cross-well (left), and CMP gather after NMO correction in surface seismic.

THE HNMO CORRECTION

The traveltime equation for a reflection in the orthogonal CLP reflection polar coordinate stacking system (Smalley, 1992), assuming constant slowness is

$$t = s\{r^2(Zr)[1 + \sin 2\alpha(Zr)] + fx^2\}^{\frac{1}{2}}, \quad (2)$$

where $r(Z_r)$ and $\alpha(Z_r)$ are the cross-well polar coordinates, Zr is the depth of the reflection, and fx is the well separation. By writing the traveltime equation in this form we can define a new set of gathers. The gathers that we want to consider for cross-well reflection velocity analysis are the CLP (Common Lateral Point) gathers. This gather is defined by holding the value $\alpha(Zr)$ constant in equation (2). A CLP gather is shown in figure 3. As is shown in figure 3 and in equation (2) the moveout is hyperbolic.

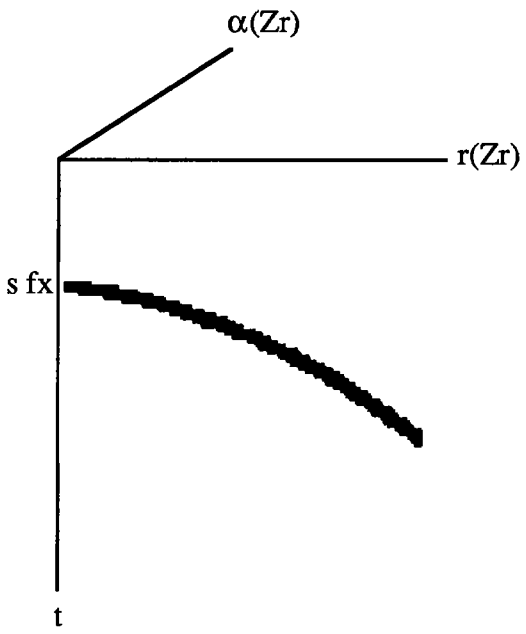

Figure 3. CLP gather.

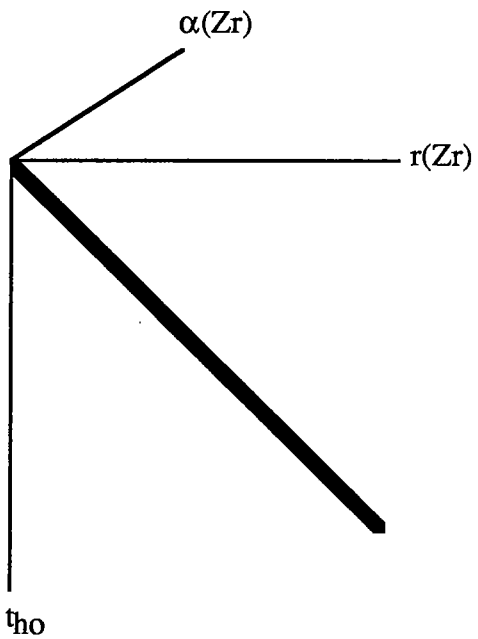

Figure 4. CLP - HNMO gather.

The first step in the two step correction to zero source - geophone offset is the HNMO correction (Horizontal Normal Moveout) (Smalley, 1992). The HNMO equation corrects for the horizontal offset of the source and geophone wells. The HNMO corrected time is

$$t_{ho} = s \cdot r(Zr)[1 + \sin 2\alpha(Zr)]^{\frac{1}{2}}, \tag{3}$$

and therefore the HNMO moveout equation is

$$t^2 = t_{ho}^2 + s^2 fx^2. \tag{4}$$

This is a non-linear moveout equation similar to the surface seismic NMO equation (equation 1). The HNMO corrected CLP gather (CLP - HNMO) is shown in figure 4. The moveout of this gather has three important characteristics:

1) it intersects the origin ($t_{ho} = 0$, $r(Zr) = 0$).

2) the moveout is linear with respect to r.

3) the slope of the line is proportional to the slowness of the medium.

All three of these quantities are mathematically clear from equation 3. The slope of the event is

$$\frac{\Delta t_{ho}}{\Delta r} = s \cdot [1 + \sin 2\alpha(Zr)]^{\frac{1}{2}}, \tag{5}$$

which can be solved for slowness:

$$s = [1 + \sin 2\alpha(Zr)]^{-\frac{1}{2}} \frac{\Delta t_{ho}}{\Delta r}. \tag{6}$$

Therefore we want to transform the data from the CLP gather (figure 3) to the CLP - HNMO gather (figure 4) by use of equation 4. The unknown is the slowness. Use of the correct slowness will do the transformation perfectly and gives us the three characteristics listed previously.

Erroneous slowness and correct reflector depth

As a first step in velocity analysis and depth conversion we want to examine what an erroneous slowness will do. We assume that we have a reflection at the assumed reflector depth. The HNMO correction can be written as

$$t_{ho}^2 = t^2 - s^2 fx^2. \tag{7}$$

In practice the slowness s will be estimated by s_o. The relationship between s and s_o is

$$s = s_o + \Delta s. \tag{8}$$

Therefore the estimated correction is

$$(t_{ho}^2)_e = t^2 - s_o{}^2 fx^2. \tag{9}$$

The relationship between the estimated HNMO corrected time $(t_{ho})_e$ and the true HNMO corrected time (t_{ho}) is

$$(t_{ho}^2)_e = t_{ho}^2 + \Delta s(2s_o + \Delta s)fx^2, \tag{10}$$

or

$$(t_{ho})_e = [t_{ho}^2 + (s^2 - s_o^2)fx^2]^{\frac{1}{2}}. \tag{11}$$

We see that the estimated HNMO corrected time is hyperbolic and doesn't meet any of the three criterion for ideal moveout. When the slowness estimate is too small ($s_O < s$) the intercept is on the t_{ho} axis (Figure 5). When the slowness estimate is too big ($s_O > s$) the intercept is on the radial distance axis (Figure 5). Therefore a reflector at the assumed reflector depth with an erroneous slowness estimate will have an estimated HNMO corrected time that does not intercept the origin and has hyperbolic moveout.

Erroneous slowness estimate and erroneous reflection depth

The variation of the moveout curve intercept with the slowness estimate gives us another

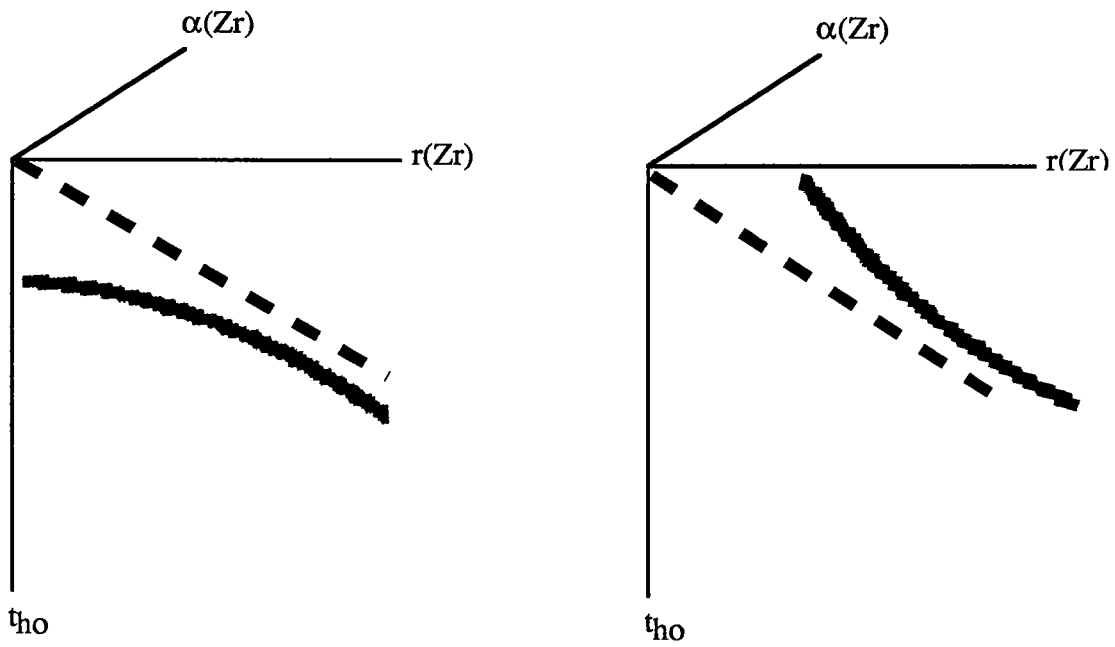

Figure 5. CLP - HNMO gathers for a reflection at the assumed reflector depth when the slowness estimate is too small ($s_0 < s$) (left), and when the slowness estimate is too large ($s_0 > s$) (right). The dashed line shows the correct moveout curve

problem. This is the ambiguity of the reflector depth and slowness. This problem can be seen by looking at the equation $\mathbf{t} = \mathbf{s} \cdot \mathbf{l}$. Looking at the traveltime gives us many possible solutions for **s** and **l**. We look to resolve this problem by considering the moveout of the reflection event. As described previously, only a reflection at the correct or assumed reflector depth with the correct HNMO slowness will result in a straight line that intersects the origin. A reflector at a depth other than the assumed reflector depth could intercept the origin for a certain erroneous slowness estimate. The error in the polar coordinate calculations for the CLP stacking coordinate system (Smalley, 1992) for a reflector at a depth other than the assumed reflector depth can be seen by comparing the sets of equations

$$\alpha(\mathrm{Zr}) = \tan^{-1}\left[\frac{\mathrm{Zr} - \mathrm{Zg}}{\mathrm{Zr} - \mathrm{Zs}}\right], \tag{12}$$

$$\mathrm{r(Zr)} = \left[(\mathrm{Zr} - \mathrm{Zg})^2 + (\mathrm{Zr} - \mathrm{Zs})^2\right]^{\frac{1}{2}}, \tag{13}$$

$$\alpha'(Zr) = \tan^{-1}\left[\frac{(Zr + \Delta Zr) - Zg}{(Zr + \Delta Zr) - Zs}\right], \tag{14}$$

$$r'(Zr) = \left\{[(Zr + \Delta Zr) - Zg]^2 + [(Zr + \Delta Zr) - Zs]^2\right\}^{\frac{1}{2}}, \tag{15}$$

where $\alpha'(Zr)$ and $r'(Zr)$ are the polar coordinate for the true reflector depth, ΔZr is the change in reflector depth relative to Zr, Zs is the depth of the source, and Zg is the depth of the geophone. Since the true reflector depth is unknown, all of the gathers will still be in terms of the original polar coordinates $\alpha(Zr)$ and r(Zr) based on the assumed reflector depth Zr. The traveltime for the actual reflection can be written as

$$\left(t'\right)^2 = \left(t'_{ho}\right)^2 + s^2 fx^2, \tag{16}$$

where

$$t'_{ho} = s \cdot r'(Zr)[1 + \sin 2\alpha(Zr)]^{\frac{1}{2}}, \tag{17}$$

We make an estimate to the slowness as before:

$$(t'_{ho})_e = [\left(t'_{ho}\right)^2 + (s^2 - s_o^2) fx^2]^{\frac{1}{2}}. \tag{18}$$

As stated before, reflections other than a reflection at the assumed reflector depth can be forced to intercept the origin by varying the slowness estimate. We can do this by letting the value under the radical in equation (18) be zero. This is accomplished when the slowness estimate has the value:

$$. s_o = \frac{s}{fx} \cdot \left\{fx^2 + \left[1 + \sin 2\alpha'(Zr)\right] \cdot (\Delta r)^2\right\}^{\frac{1}{2}} \tag{19}$$

where

$$\Delta r = r' - r \tag{20}$$

When this value is used for the slowness estimate, the HNMO corrected time of this reflector $(t_{ho}')_e$ is

$$(t_{ho}')_e = s \cdot \left\{ \left[1 + \sin 2\alpha'(Zr) \right] \cdot \left[r^2 + 2r\Delta r \right] \right\}^{\frac{1}{2}} \tag{21}$$

We can see that a reflector other than a reflector at the assumed reflector depth will be hyperbolic if we force the intercept to be at the origin (Figure 6). This characteristic is very important in separating the depth of the reflection from the slowness of the medium. The moveout of the event tells us if we have the correct event (i.e. a reflection at the assumed reflector depth). Only an event that intercepts the origin with linear moveout is located at the assumed reflector depth.

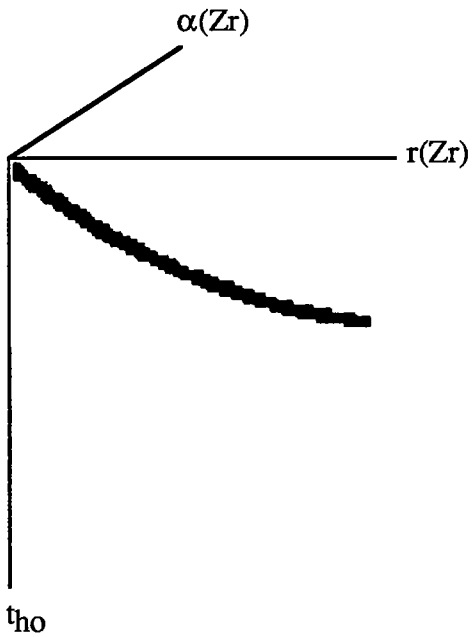

Figure 6. CLP - HNMO gather showing moveout curve for a reflection at a depth other than the assumed reflector depth, but intersecting the origin due to use of a certain incorrect slowness. It is distinguished from a reflection at the assumed reflector depth by its hyperbolic moveout.

Correct slowness and incorrect reflector depth

If we use the correct slowness but the reflection event is at a depth other than the assumed reflector depth the traveltime equation is

$$(t'_{ho}) = s \cdot \left[1 + \sin 2\alpha'(Zr)\right]^{\frac{1}{2}} \cdot \left[r'(Zr + \Delta Zr)\right]. \quad (22)$$

Using equation (20), we can rewrite equation (22) as

$$(t'_{ho}) = s \cdot \left[1 + \sin 2\alpha'(Zr)\right]^{\frac{1}{2}} \cdot \left[r(Zr) + \Delta r\right] \quad (23)$$

Because Δr depends on r in a non- linear fashion (equations (13) and (15)):

$$\Delta r = f(r, \Delta Zr, Zg, Zs) \quad (24)$$

equation (23) is hyperbolic. If the reflection has a smaller radial distance than the assumed reflector depth, the intercept will be on the radial distance axis (Figure 7). If the reflection has a larger radial distance than the assumed reflector depth, the intercept will be on the time (t_{ho}) axis (Figure 7).

Therefore the ambiguity between reflector depth and slowness is resolved by the shape and intercept of the CLP-HNMO gather. Only a reflection at the assumed reflector depth with the correct slowness estimate will yield a straight line intercepting the origin; the slope of which is proportional to the slowness. This is similar to the surface seismic NMO correction in which the shape of the curve is the determining factor in obtaining the correct NMO velocity.

Synthetic Example

A synthetic seismogram was generated based on a constant slowness model of 1/12.5 ms/ft using downgoing reflections. Figure S1 shows a CLP gather where the lateral point is halfway between the wells. This corresponds to $\alpha=\pi/4$ in the polar coordinate calculations, and a ratio (relative source and geophone depth relative to the assumed reflector depth) of

one. The assumed reflector depth used in the polar coordinate calculations is 1850 ft., the same as the depth of the first reflection. Figure S2 shows a CLP - HNMO gather with an

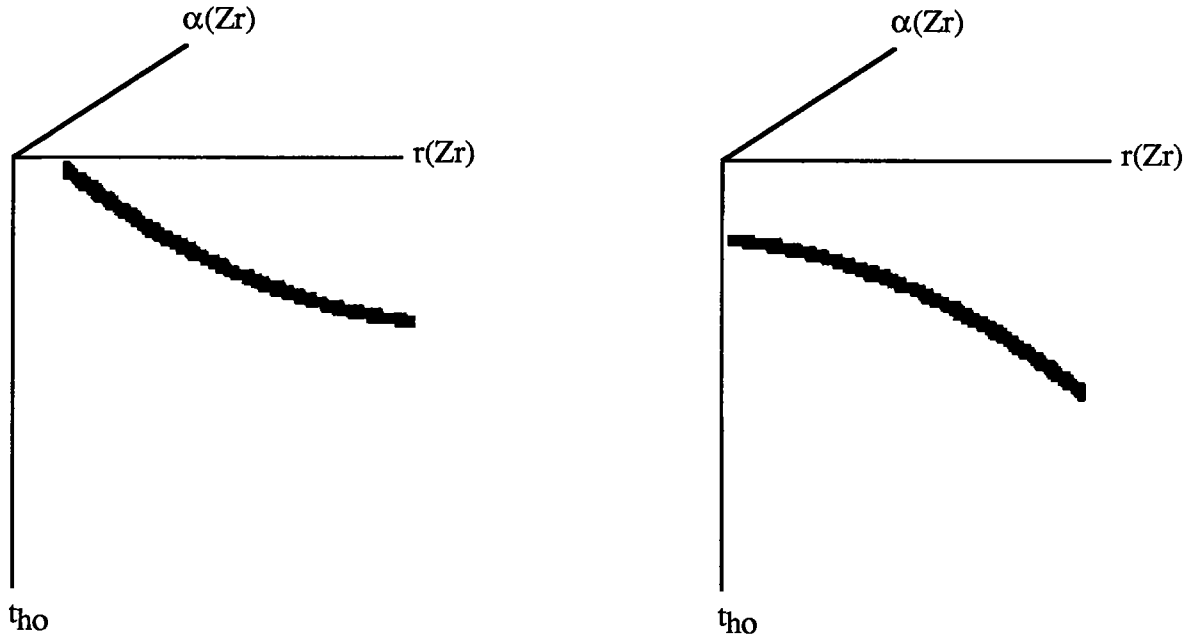

Figure 7. CLP - HNMO gathers for corrections of reflections at depths other than the the assumed reflector depth using the correct slowness. The case of a reflector with a smaller radial distance for a given lateral point than the assumed reflector depth (left), and for a larger radial distance (right). Both have hyperbolic moveouts.

HNMO slowness of 1/12.0 ms/ft. Figure S3 shows a CLP - HNMO gather with an HNMO slowness of 1/13.0 ms/ft. Figure S4 shows a CLP - HNMO gather with the correct HNMO slowness of 1/12.5 ms/ft. In this case the event intersects the origin and has linear moveout. Figure S5 shows a CLP - HNMO gather with a slowness of 1/7.1 ms/ft. This slowness is significant because it forces the reflection at 1725 ft. to intercept the origin. It is by its hyperbolic moveout that we know that the depth of this reflection is not at the assumed reflector depth, and therefore we separate depth from slowness.

THE VLMO CORRECTION

The next step in the imaging procedure is to correct for the vertical offset of the sources and geophones. This vertical offset correction is referenced to a horizontal plane at a fixed depth. This correction was defined as the VLMO correction (Vertical Linear Moveout) (Smalley, 1992). Previously, this reference plane was defined to be a depth other than the assumed reflector depth. The following equations will be based on a reference plane at the

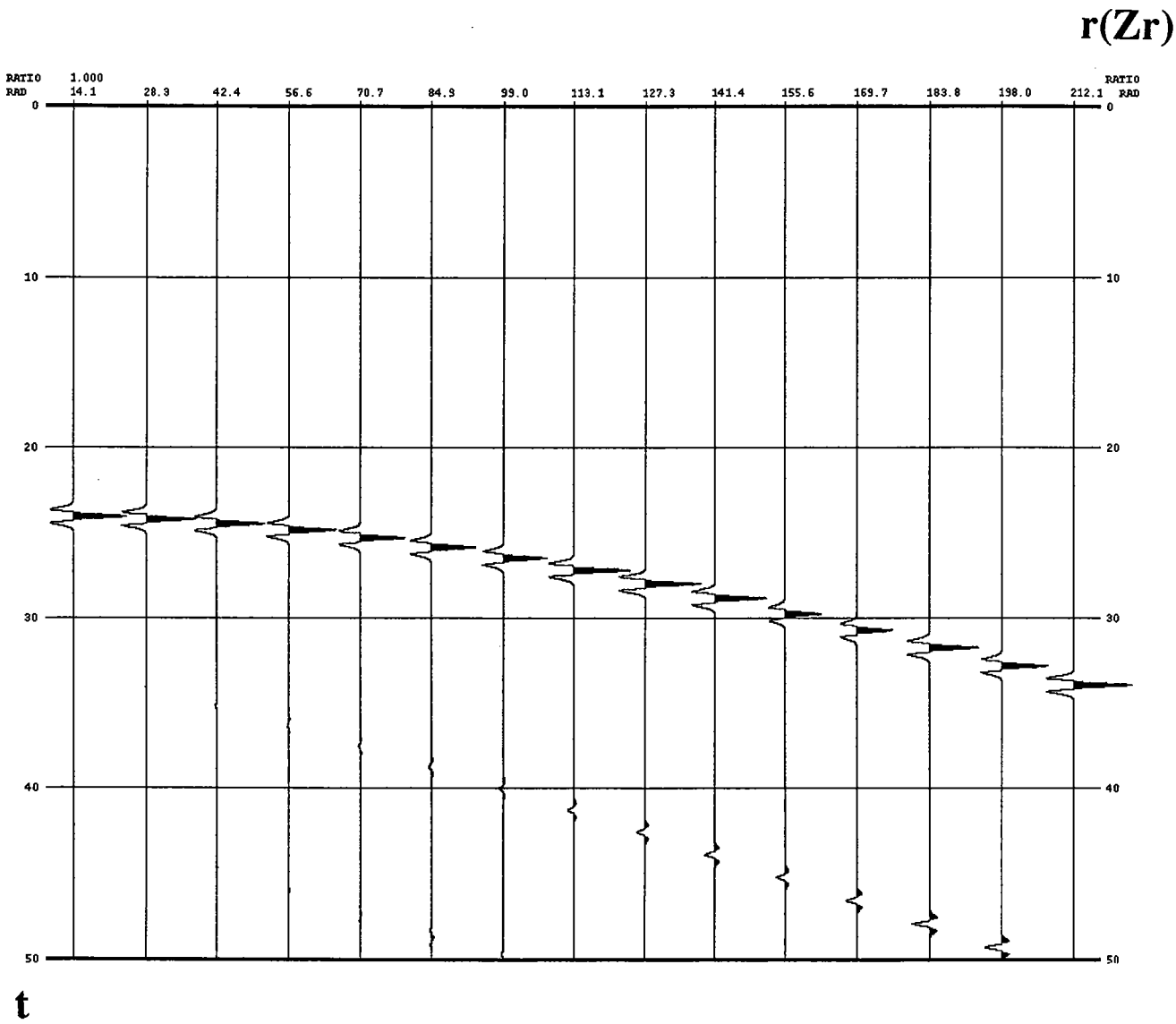

Figure S1. CLP gather for the lateral point midway between the wells.

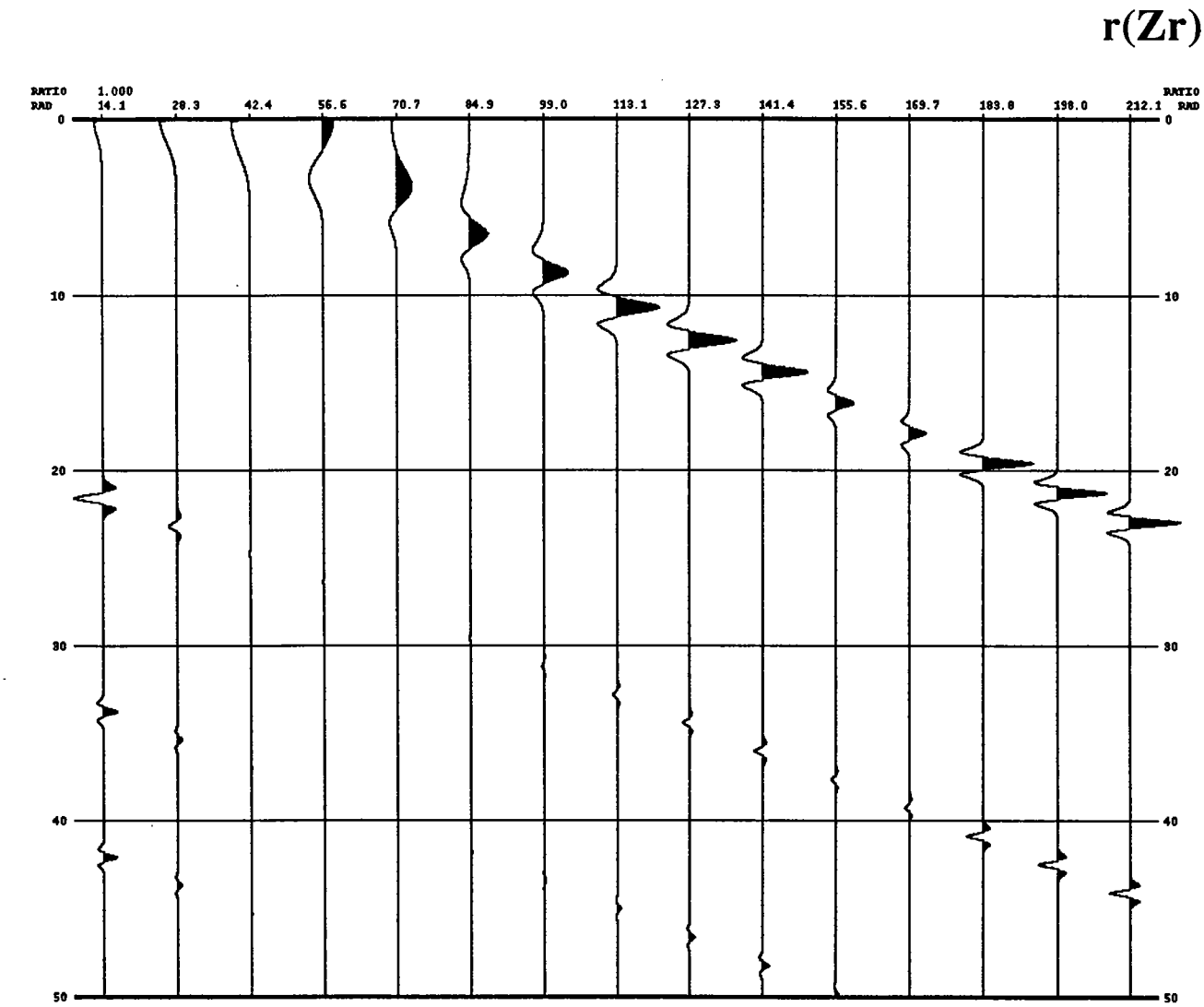

Figure S2. CLP - HNMO gather using an HNMO slowness of 1/12.0 ms/ft.

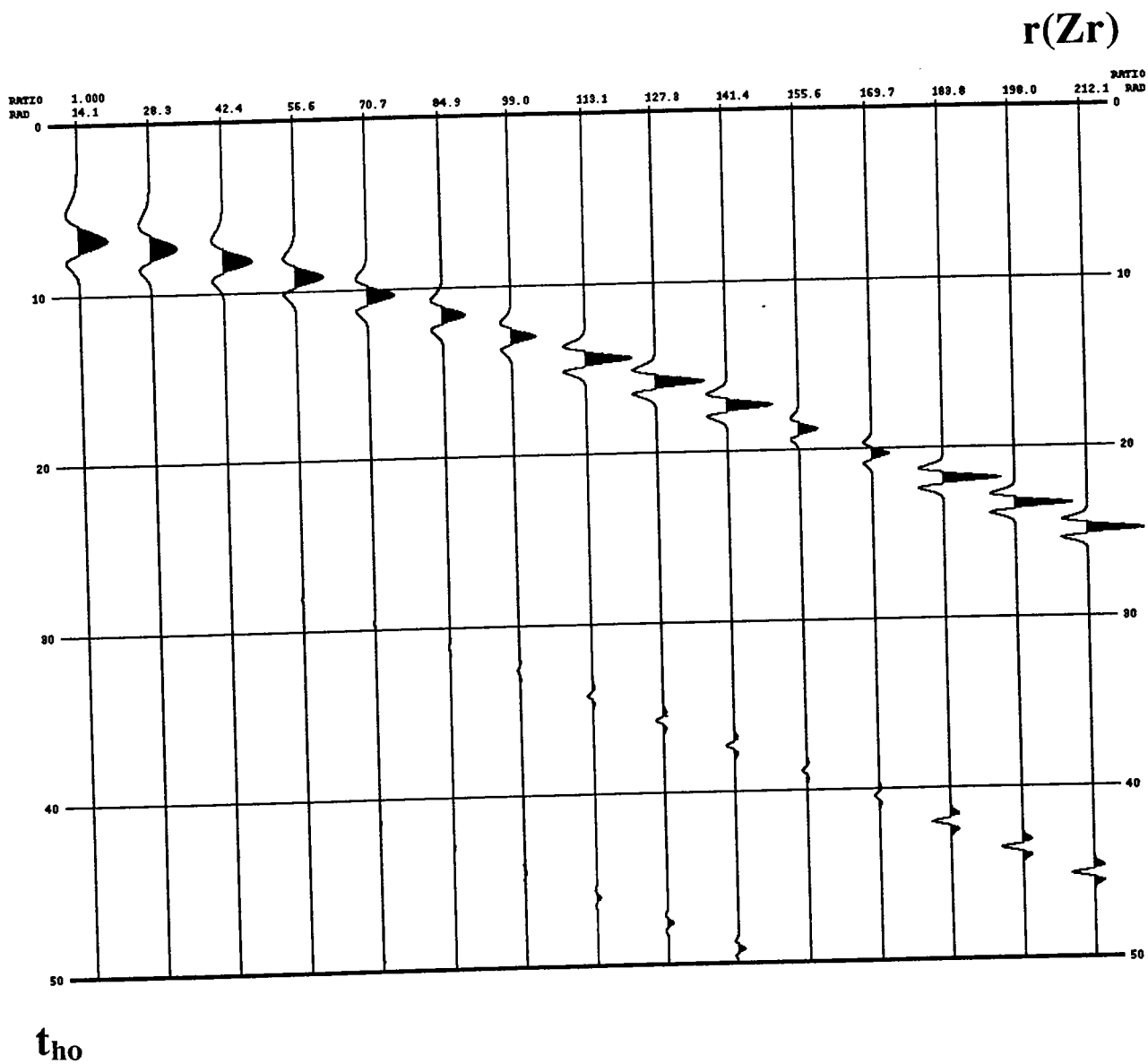

Figure S3. CLP - HNMO gather using an HNMO slowness of 1/13.0 ms/ft.

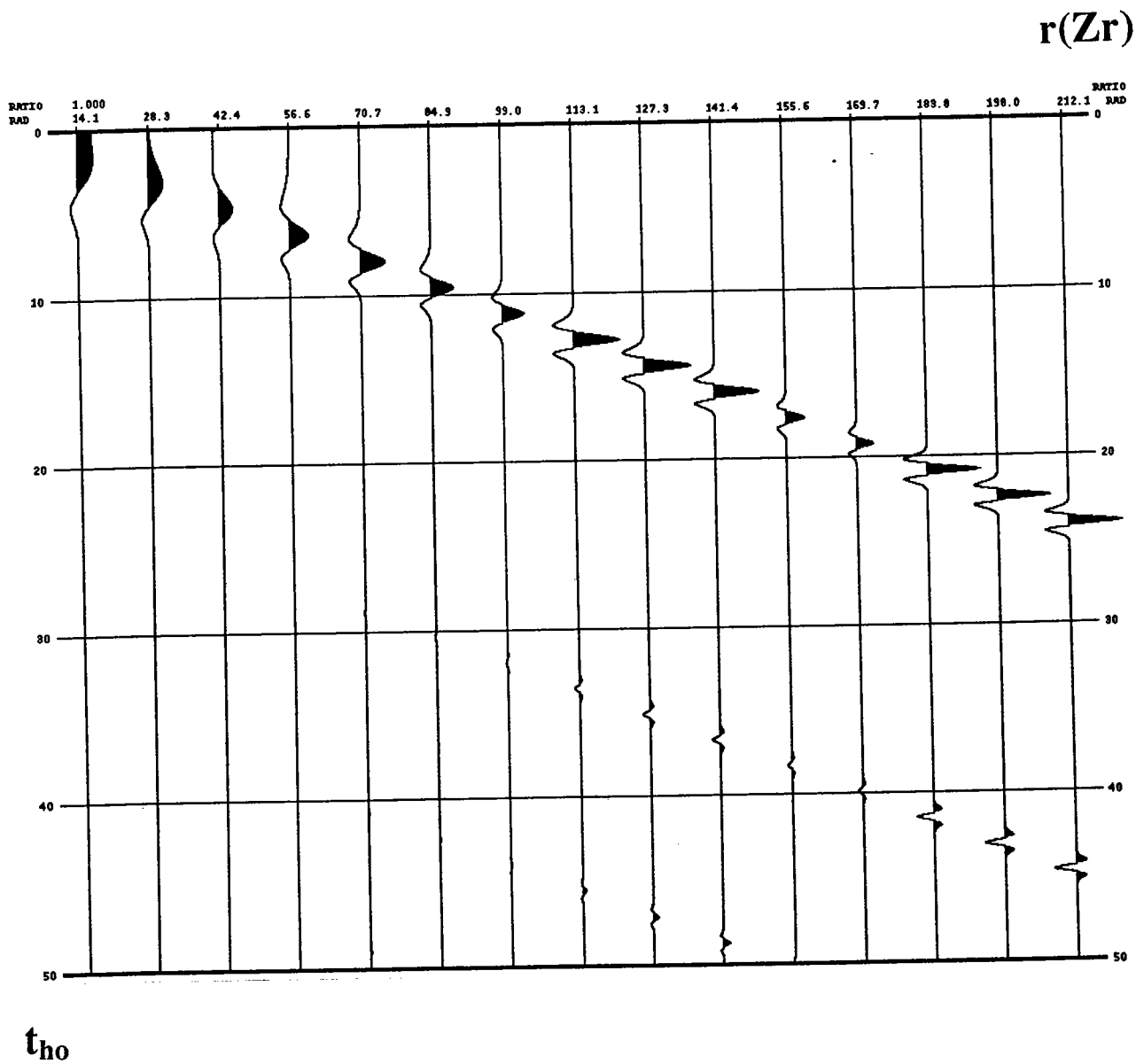

Figure S4. CLP - HNMO gather using an HNMO slowness of 1/12.5 ms/ft.

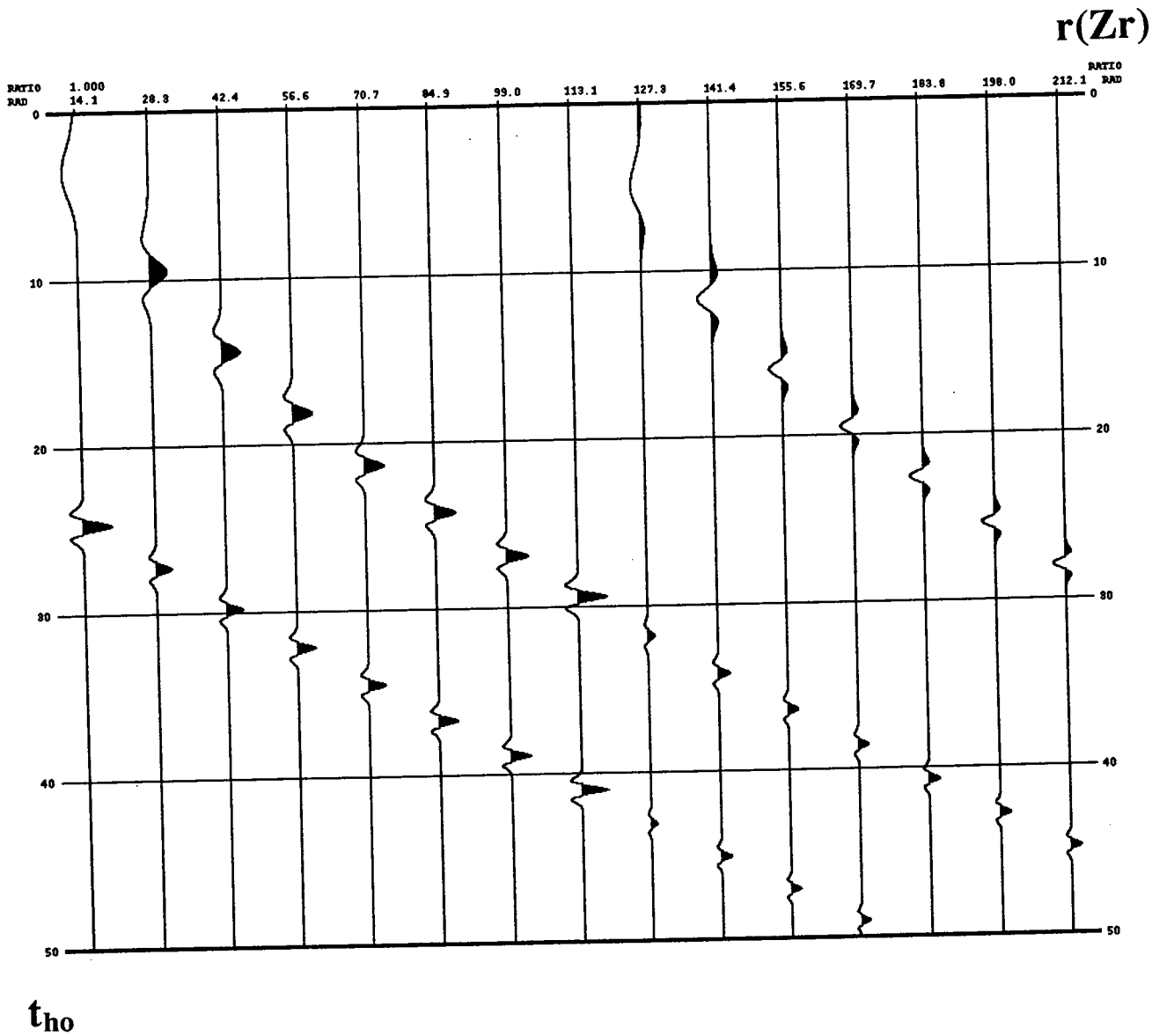

Figure S5. CLP - HNMO gather using an HNMO slowness of 1/7.1 ms/ft.

assumed reflector depth. This means that the vertical location of all source - geophone pairs will be corrected to the assumed reflector depth. Two reasons for having the reference plane at the assumed reflector depth are

1) it gives a clearer meaning to the slowness s in the VLMO equation.

2) it simplifies the process of depth conversion.

Therefore the VLMO corrected data (which always follows the HNMO corrected data) will have a traveltime of zero (figure 8). Therefore the VLMO moveout equation will have the form

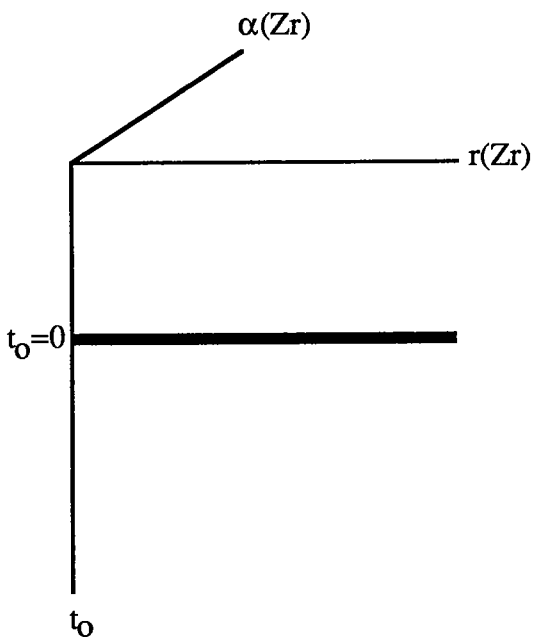

Figure 8. CLP - VLMO gather.

$$t_{ho} = t_o + s \cdot \left[1 + \sin 2\alpha(Zr)\right]^{\frac{1}{2}} \cdot r(Zr), \tag{25}$$

where $t_o = 0$. Following a process similar to the HNMO correction, we want to transform the CLP - HNMO data in figure 3 to the CLP - VLMO data in figure 8 by use of equation (25). The VLMO correction is

$$t_o = t_{ho} - s \cdot [1 + \sin 2\alpha(Zr)]^{\frac{1}{2}} \cdot r(Zr), \tag{26}$$

where again $t_o = 0$. As with the HNMO correction, we estimate the slowness s by s_o (we actually know the slowness from the HNMO correction and from the slope of the CLP - HNMO gather, but we want to examine the effect of an error in the VLMO slowness). The relationship between s and s_o is given by equation (8). The estimated VLMO correction is:

$$t_e = t_{ho} - s_o \cdot [1 + \sin 2\alpha(Zr)]^{\frac{1}{2}} \cdot r(Zr), \tag{27}$$

which is rewritten as

$$t_e = \Delta s \cdot [1 + \sin 2\alpha(Zr)]^{\frac{1}{2}} \cdot r(Zr). \tag{28}$$

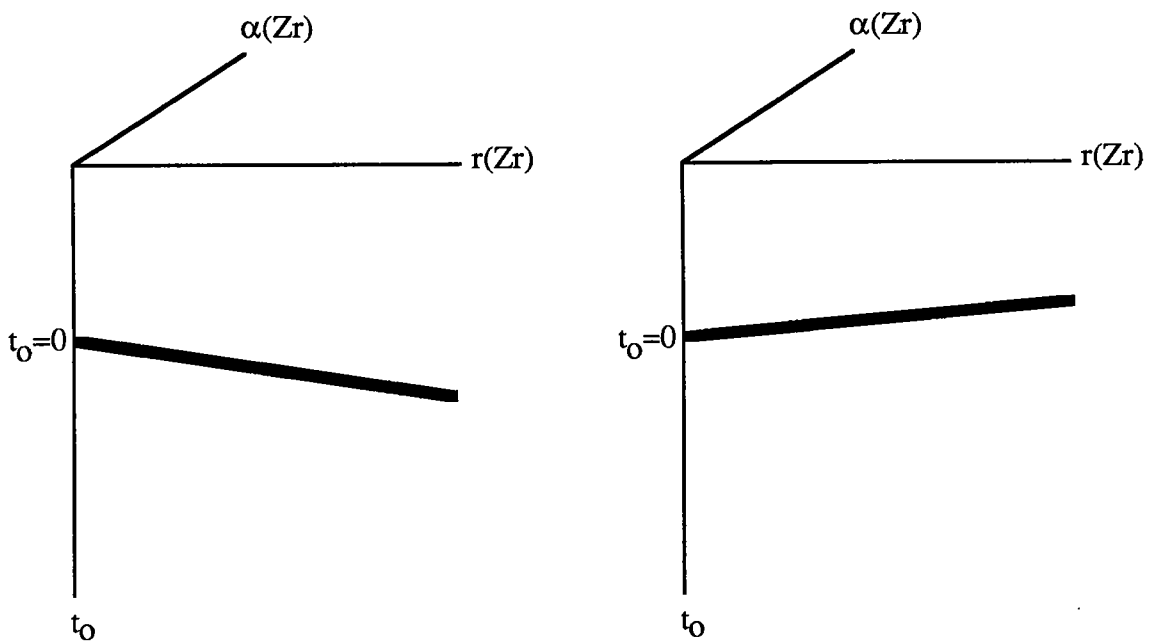

Figure 9. CLP - VLMO gathers for VLMO slowness estimates that are too small (left) and too large (right). The moveout is linear and hinged about $t_0 = 0$. The data are bulked shifted before the VLMO correction so that causality is not violated.

We see that the estimated VLMO time $(t_{ho})_e$ is a straight line hinged at the origin (t=0, r=0). The slope of the line is proportional to the error in the slowness estimate. If the slowness estimate is too small, the residual slope is positive (Figure 9). If the slowness estimate is too large, the residual slope is negative (Figure 9). The data are bulk shifted in time before the VLMO correction. Therefore causality is not violated.

Synthetic Example

Synthetic examples based on the same model as before are shown. These synthetics are CLP - VLMO gathers, and all follow the CLP - HNMO gather in figure S4 where the correct HNMO slowness was used for the correct reflector depth. Figure S6 shows a CLP - VLMO gather with a VLMO slowness of 1/12.0 ms/ft. Figure S7 shows a CLP - VLMO gather with a VLMO slowness of 1/13.0 ms/ft. Figure S8 shows a CLP - VLMO gather with the correct VLMO slowness of 1/12.5 ms/ft.

VARIABLE SLOWNESS HNMO AND VLMO CORRECTIONS

In dealing with real data, we generally never have constant velocity or slowness. We have different source - geophone pairs transversing layers of different slownesses (Figure 10). Therefore it would be more accurate to use different HNMO and VLMO velocities for source - geophone pairs that reside in layers of contrasting slowness. However, we still have not fully treated the variable slowness problem. Different source - geophone pairs that transverse the same general regions of slowness or velocity variation will still have different HNMO and VLMO stacking velocities or slownesses, due to their different vertical raypath lengths in the same layers. To accurately deal with velocity analysis of cross-well reflections, we must consider how equations (4) and (25) change for variable velocity media. These equations are (Smalley, 1992)

$$t^2 = t_{ho}^2 + C_1 fx^2 + C_2 fx^4 + \cdots + C_N fx^{2N}, \tag{29}$$

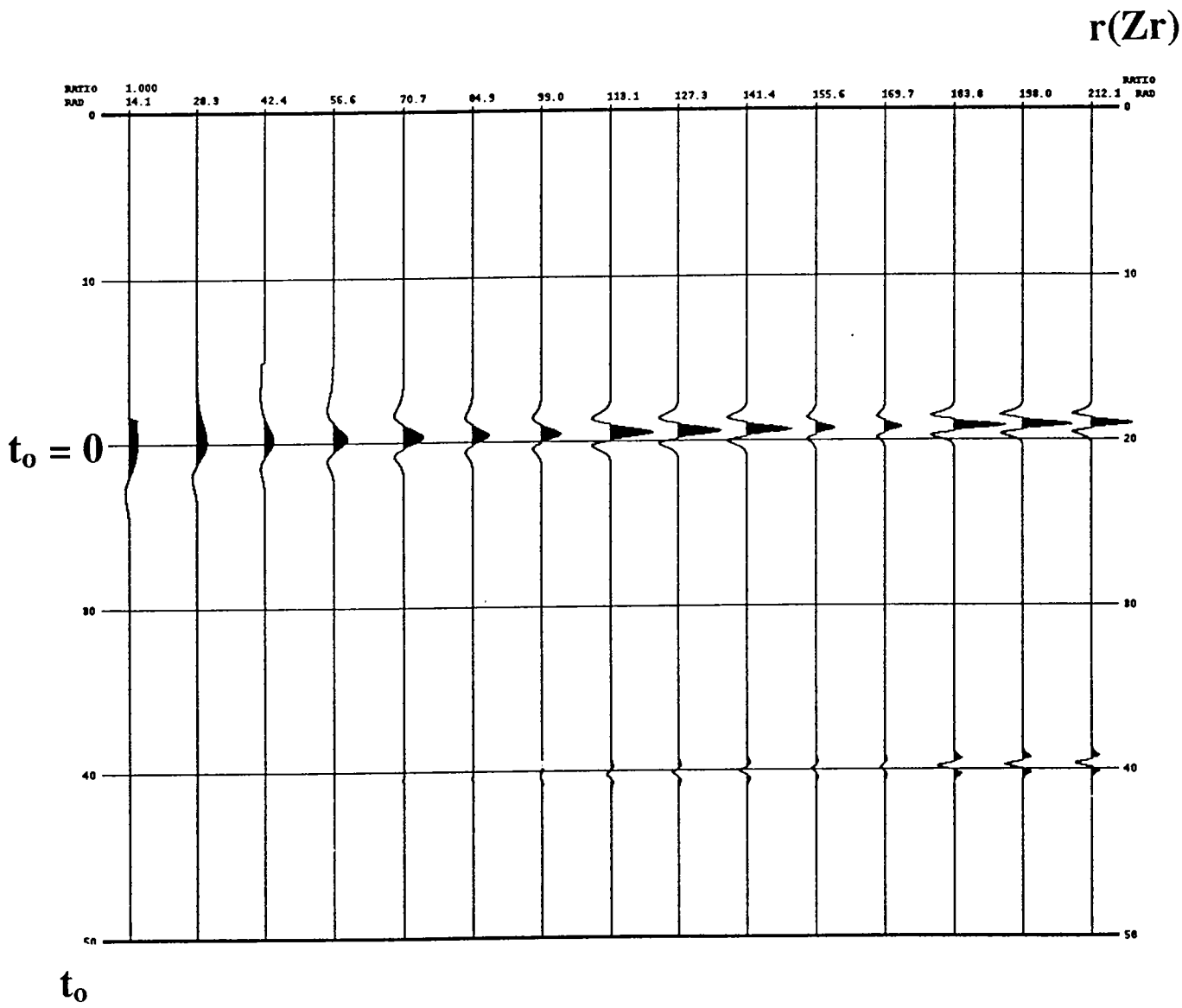

Figure S6. CLP - VLMO gather using a VLMO slowness of 1/12.0 ms/ft.

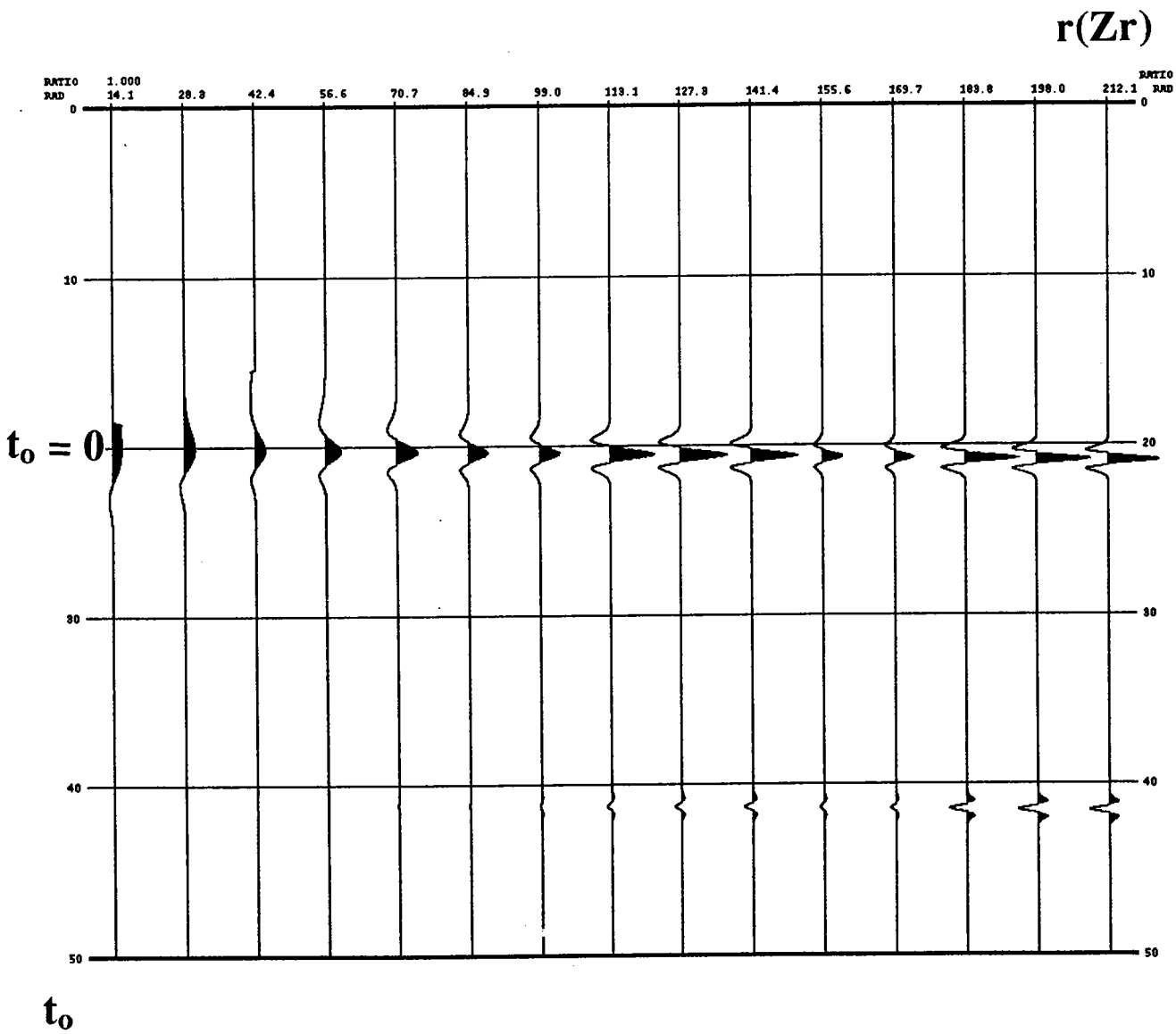

Figure S7. CLP - VLMO gather using a VLMO slowness of 1/13.0 ms/ft.

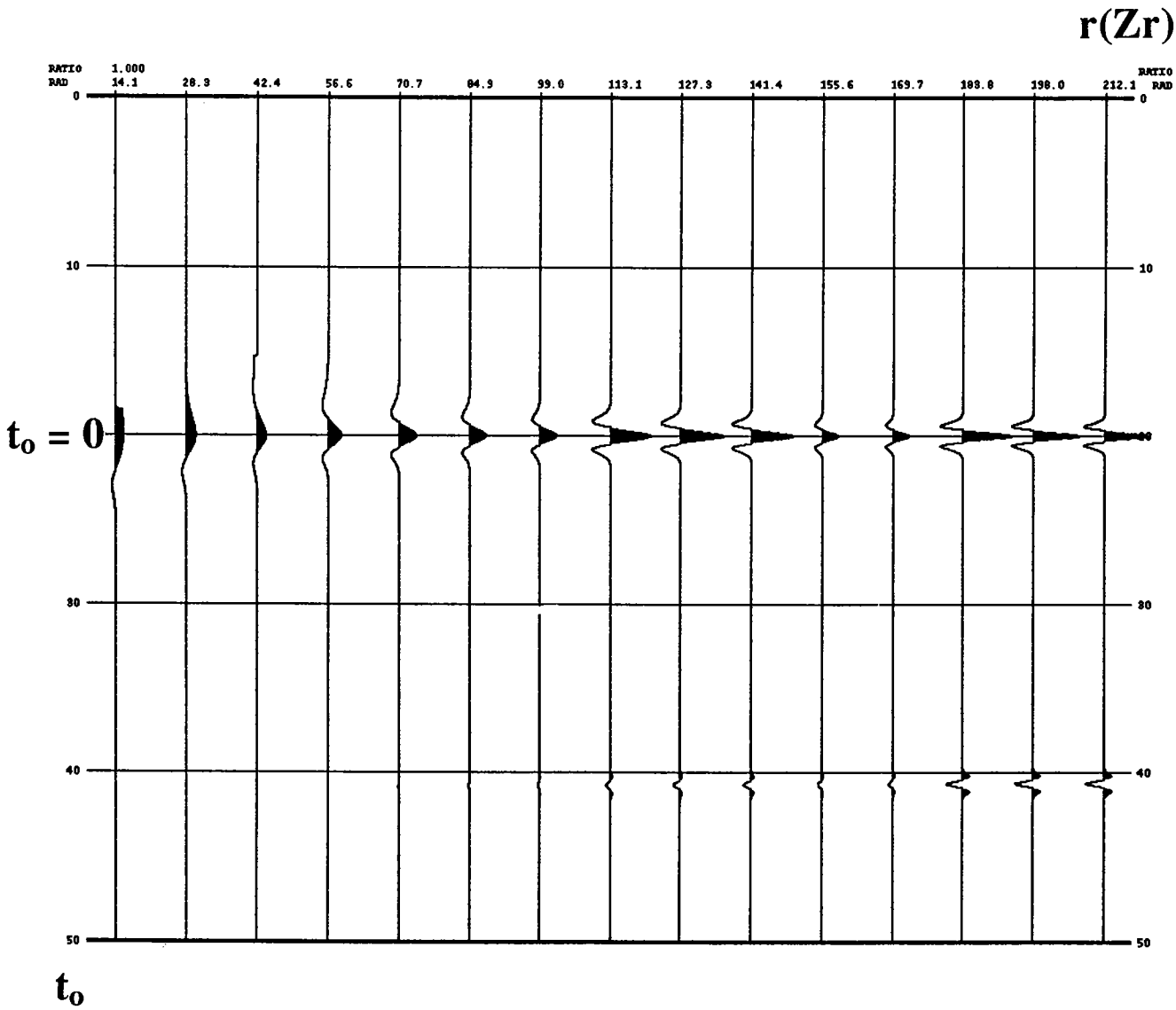

Figure S8. CLP - VLMO gather using a VLMO slowness of 1/12.5 ms/ft.

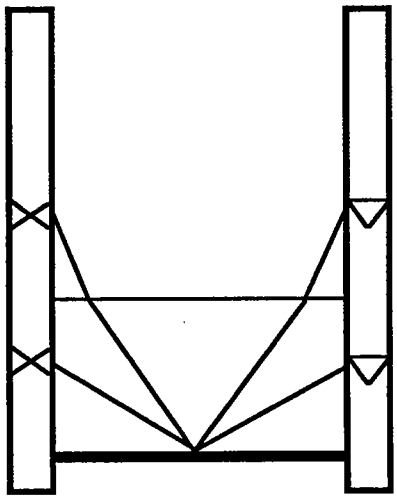

Figure 10. A cross-well common ratio gather or common lateral point gather. These source - geophone pairs transverse different layers.

where

$$C_1 = \frac{\sum_{Z=Zs}^{Z=Zr} s_i \Delta z_i + \sum_{Z=Zg}^{Z=Zr} s_i \Delta z_i}{\sum_{Z=Zs}^{Z=Zr} \frac{\Delta z_i}{s_i} + \sum_{Z=Zg}^{Z=Zr} \frac{\Delta z_i}{s_i}}, \tag{30}$$

and

$$t_{ho} = \sum_{Z=Zs}^{Z=Zr} s_i \Delta z_i + \sum_{Z=Zg}^{Z=Zr} s_i \Delta z_i, \tag{31}$$

where s_i is the interval slowness, and Δz_i is the interval thickness. C_1 is also equivalent to the inverse of the RMS velocity squared of the transversed layers. Equation (29) is the variable velocity HNMO equation, and equation (31) is the variable velocity VLMO equation. Equation (29) is similar to the surface seismic expansion about zero source - geophone offset. In the cross-well case, we expand in terms of zero well offset. In surface seismic, this equation is usually truncated after the second term, which is reasonable when

the offset is small when compared to reflection depth. For cross-well we will also truncate this equation after two terms, with the justification being that when the slowness change is small, this approximation is also quite accurate. In cross-well we look at much smaller depth ranges, and therefore the overall slowness gradient for a CLP gather is usually much smaller than a surface seismic CDP gather. Equation (31) is unique in that there is no corresponding equation in surface seismic. We can rewrite equation (31) as

$$t_{ho} = \bar{s} \cdot \left[1 + \sin 2\alpha(Zr)\right]^{\frac{1}{2}} \cdot r(Zr) \tag{32}$$

where $\bar{s}$ is the average slowness, defined by

$$\bar{s} = \frac{1}{\left[|Zr - Zs| + |Zr - Zg|\right]} \left(\sum_{Z=Zs}^{Z=Zr} s_i \Delta z_i + \sum_{Z=Zg}^{Z=Zr} s_i \Delta z_i \right) \tag{33}$$

We can compare the coefficients C1**1/2 and $\bar{s}$. These values both have units of slowness. Some simple algebra shows that

$$C1^{**}1/2 \leq \bar{s} \ . \tag{34}$$

The variable velocity analysis problem in cross-well is more complicated than in surface seismic. We can not assign one HNMO or VLMO slowness to all source - geophone pairs for a given reflection as in surface seismic. Every source - geophone pair will have a different set of HNMO and VLMO stacking slownesses for a given reflector depth, except those whose corresponding raypaths transverse only one slowness. This makes the cross-well velocity analysis problem cumbersome. However, we can simplify the problem by looking at different regions of radial distances for each lateral point that is considered for velocity analysis as opposed to every individual source - geophone pair (Figure 11). These regions usually represent regions of constant slowness, where the slowness varies only slightly, or where the slowness changes in a systematic way, such as linearly. By considering different regions of radial distances, we are breaking the problem down into a series of slowness corrections in terms of the ideal shape of the moveout curve. However, for reasons described previously we cannot assign one HNMO or VLMO slowness for each of these regions. However, we will see that we can assign one residual slowness

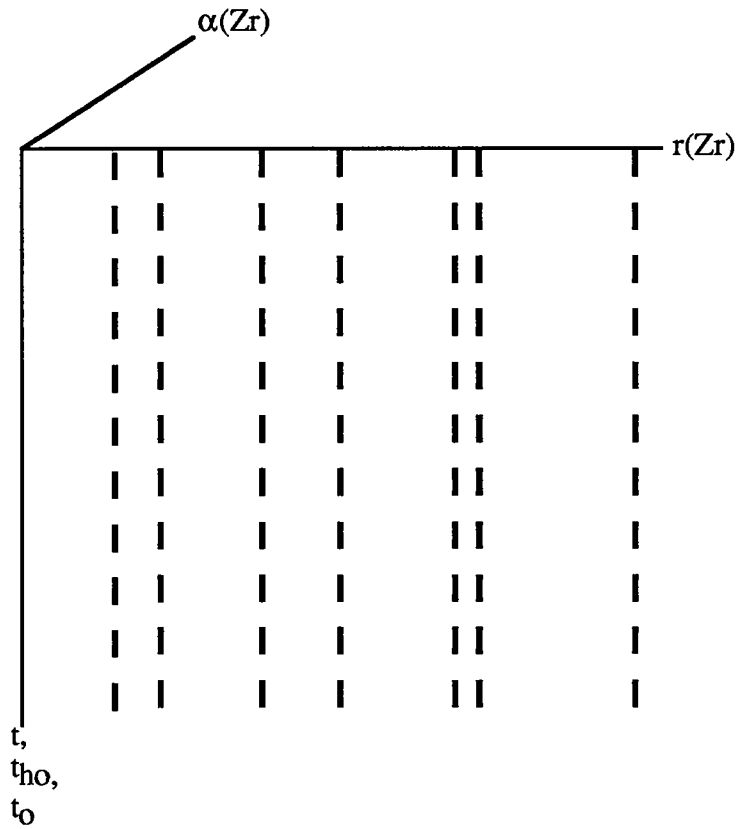

Figure 11. A breakdown of the CLP gather into regions of radial distances. These divisions represent regions of constant slowness, near constant slowness, or where the slowness changes linearly. The CLP, CLP - HNMO, and CLP - VLMO gathers will indicate the location and size of the divisions.

correction to each of these regions, with the changing HNMO and VLMO velocities calculated automatically by a radial distance gradient. The CLP, CLP-HNMO, and CLP-VLMO gathers should help suggest the number and extent of these regions. The first region that is considered starts at radial distance zero. Each time we apply a correction, that correction is applied to the entire CLP gather. Therefore as we progress through increasing radial distances, we will be making a series of residual corrections. Figure 12 shows CLP gather in a variable slowness medium. We see several hyperbolas with different asymptotes. These changes in hyperbolic shape indicate the individual radial distance regions that should be used in the velocity analysis sequence. These changes in the moveout curvature can be quite subtle in the real data.

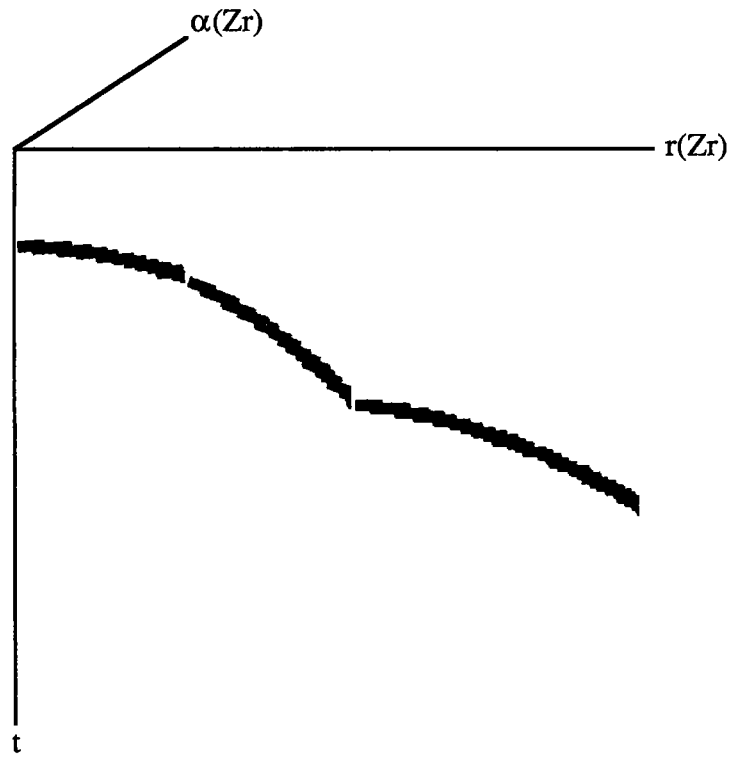

Figure 12. CLP gather for variable slowness media.

VARIABLE SLOWNESS HNMO CORRECTION

Now lets consider HNMO corrected time in a variable slowness medium. If we consider the first source geophone pair shown in figure 10, its HNMO corrected time, (t_{ho}) is

$$t_{ho} = \bar{s} \cdot \left[1 + \sin 2\alpha(Zr)\right]^{\frac{1}{2}} \cdot r(Zr). \tag{35}$$

The second source - geophone pair HNMO corrected time will be

$$t'_{ho} = \sum_{Z=Zs}^{Z=Zr} s_i \Delta z_i + \sum_{Z=Zg}^{Z=Zr} s_i \Delta z_i + \sum_{Z=Zs}^{Z=Zs'} s_i \Delta z_i + \sum_{Z=Zg}^{Z=Zg'} s_i \Delta z_i , \tag{36}$$

which can be rewritten as

$$t'_{ho} = \bar{s}' \cdot \left[1 + \sin 2\alpha(Zr)\right]^{\frac{1}{2}} \cdot r'(Zr), \tag{37}$$

where $\bar{s}'$ and $r'(Zr)$ are the average slowness and radial distance relative to the assumed reflector depth for the second source - geophone pair. We see that the HNMO corrected time of the second source - geophone pair adds linearly to the HNMO correction of the first source - geophone pair:

$$t'_{ho} = t_{ho} + \sum_{Z=Zs}^{Z=Zs'} s_i \Delta z_i + \sum_{Z=Zg}^{Z=Zg'} s_i \Delta z_i , \tag{38}$$

which can be rewritten as

$$t_{ho} = [\bar{s} \cdot r(Zr) + \bar{s}_{\Delta r} \cdot \Delta r(Zr)] \cdot [1 + \sin 2\alpha(Zr)]^{\frac{1}{2}}, \tag{39}$$

where

$$\Delta r = r' - r , \tag{40}$$

and

$$\bar{s}_{\Delta r} = \frac{1}{\left[\left|Zs' - Zs\right| + \left|Zg' - Zg\right|\right]} \cdot \left(\sum_{Z=Zs}^{Z=Zs'} s_i \Delta z_i + \sum_{Z=Zg}^{Z=Zg'} s_i \Delta z_i \right). \tag{41}$$

The CLP - HNMO gather is a series of line segments that is continuous, but with different slopes (Figure 13). We can see this mathematically if we take the derivative of equation (39) with respect to r:

$$\frac{dt'_{ho}}{dr} = \bar{s} \cdot [1 + \sin 2\alpha(Zr)]^{\frac{1}{2}}, \tag{42}$$

and with respect to Δr

$$\frac{dt'_{ho}}{d\Delta r} = \bar{s}_{\Delta r} \cdot [1 + \sin 2\alpha(Zr)]^{\frac{1}{2}}. \tag{43}$$

We can also see that the slope for each regions of the radial distance is proportional to the average slowness for the given radial distance region.

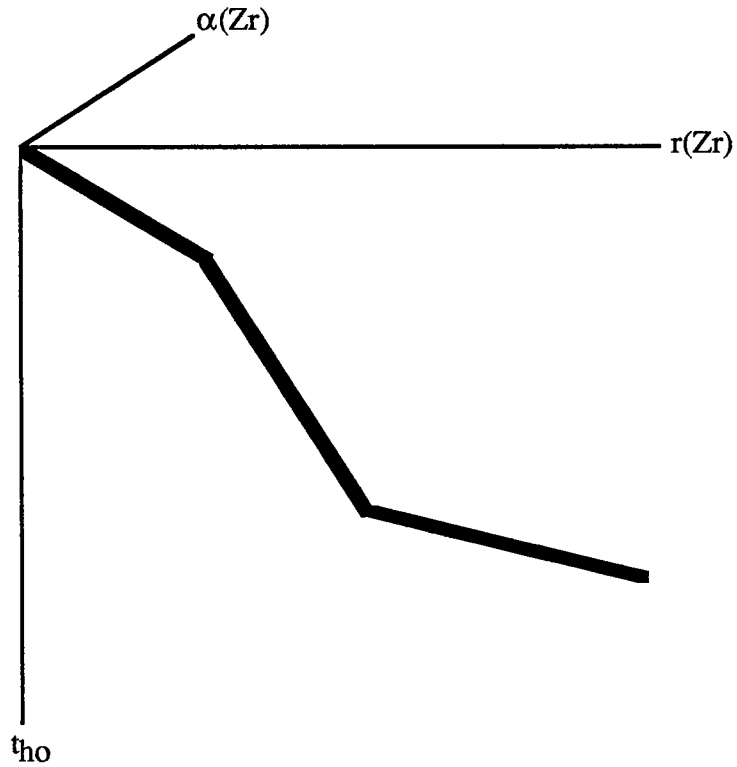

Figure 13. CLP - HNMO gather for variable slowness media.

Let us again consider the two source - geophone pairs shown in figure 10. The RMS velocity for the first source - geophone pair is

$$RMS^2 = \frac{\sum_{Z=Zs}^{Z=Zr} \frac{\Delta z_i}{s_i} + \sum_{Z=Zg}^{Z=Zr} \frac{\Delta z_i}{s_i}}{\sum_{Z=Zs}^{Z=Zr} s_i \Delta z_i + \sum_{Z=Zg}^{Z=Zr} s_i \Delta z_i}. \tag{44}$$

The RMS velocity for the second source - geophone pair is

$$\left(RMS'\right)^2 = \frac{\sum_{Z=Zs}^{Z=Zr} \frac{\Delta z_i}{s_i} + \sum_{Z=Zg}^{Z=Zr} \frac{\Delta z_i}{s_i} + \sum_{Z=Zs}^{Z=Zs'} \frac{\Delta z_i}{s_i} + \sum_{Z=Zg}^{Z=Zg'} \frac{\Delta z_i}{s_i}}{\sum_{Z=Zs}^{Z=Zr} s_i \Delta z_i + \sum_{Z=Zg}^{Z=Zr} s_i \Delta z_i + \sum_{Z=Zs}^{Z=Zs'} s_i \Delta z_i + \sum_{Z=Zg}^{Z=Zg'} s_i \Delta z_i}. \tag{45}$$

We define the following expression for the RMS velocity of the layers transversed by the second source - geophone pair but not the first as:

$$RMS^2_{\Delta r} = \frac{\sum_{Z=Zs}^{Z=Zs'} \frac{\Delta z_i}{s_i} + \sum_{Z=Zg}^{Z=Zg'} \frac{\Delta z_i}{s_i}}{\sum_{Z=Zs}^{Z=Zs'} s_i \Delta z_i + \sum_{Z=Zg}^{Z=Zg'} s_i \Delta z_i}. \tag{46}$$

When we find the optimum HNMO velocity for the first source - geophone pair, we apply that correction for all radial distances, and therefore the second source - geophone pair. We need to do a residual correction to find the optimum HNMO velocity for the second source - geophone pair. We can rewrite the RMS velocity for the second source - geophone pair in terms of the RMS velocity for the first source - geophone pair.

$$\left(RMS'\right)^2 = RMS^2 + \frac{\bar{s}_{\Delta r}}{\bar{s}} \left(\frac{1}{1 + \frac{\bar{s}_{\Delta r}}{\bar{s}} \frac{\Delta r}{r}} \right) \frac{\Delta r}{r} \cdot \Delta RMS \tag{47}$$

where

$$\Delta RMS = RMS^2_{\Delta r} - RMS^2, \tag{48}$$

where $\bar{s}$ is the average slowness of the medium over the vertical raypath extent of the first source - geophone pair, and r is the radial distance relative to the assumed reflector depth of the first source - geophone pair. We can make the following approximation if the velocity contrast is small by using a Taylor series expansion:

$$\left(RMS'\right)^2 = RMS^2 + \left(\frac{\bar{s}_{\Delta r}}{\bar{s}} \frac{\Delta r}{r} \right) \cdot \Delta RMS. \tag{49}$$

Using another Taylor Series Expansion approximation we obtain a residual correction that is linear with increasing radial distance:

$$RMS' = RMS \left[1 + \frac{1}{2} \left(\frac{\bar{s}_{\Delta r}}{\bar{s}} \frac{\Delta r}{r} \right) \cdot \frac{\Delta RMS}{RMS^2} \right]. \tag{50}$$

Synthetic Example

A synthetic example for a variable slowness synthetic data set is shown. A CLP gather for the midpoint between the wells is shown in figure S9. There is some interference with the direct arrival for small radial distances within this synthetic data set. A CLP - HNMO gather is shown after a single HNMO slowness has been applied (Figure S10). The CLP - HNMO gather after the full sequence of residual HNMO rms velocities have been applied is shown in figure S11.

VARIABLE SLOWNESS VLMO CORRECTION

The VLMO corrected data (CLP - VLMO) is the same as the constant slowness case (Figure 14). Once again considering the two source - geophone pairs in figure 10, we showed in equations (35) and (37) the HNMO corrected traveltimes for these source - geophone pairs. Since the VLMO corrected time is zero, these equations are equivalent to the correction that is applied to transform the data from HNMO corrected time (Figure 13) to VLMO corrected time (Figure 14). The variable slowness VLMO correction is carried out the same way as the variable slowness HNMO correction . We start at r=0 and progress to larger values of r; each correction that is done is applied to all r. Therefore we do a series of residual slowness corrections. Similar to the HNMO correction we need to find the residual VLMO correction for the second source - geophone pair in figure 10 when it is corrected for the optimum slowness of the first source - geophone pair in figure 10. Using equation (39), We can write the VLMO correction for the second source- geophone pair in terms of the optimum slowness for the first source - geophone pair with an error term:

$$t'_{ho} = \left(\bar{s} + \frac{\Delta r}{r'} \Delta s \right) r' \cdot [1 + \sin 2\alpha (Zr)]^{\frac{1}{2}}, \tag{51}$$

where

$$\Delta \bar{s} = \bar{s}_{\Delta r} - \bar{s}. \tag{52}$$

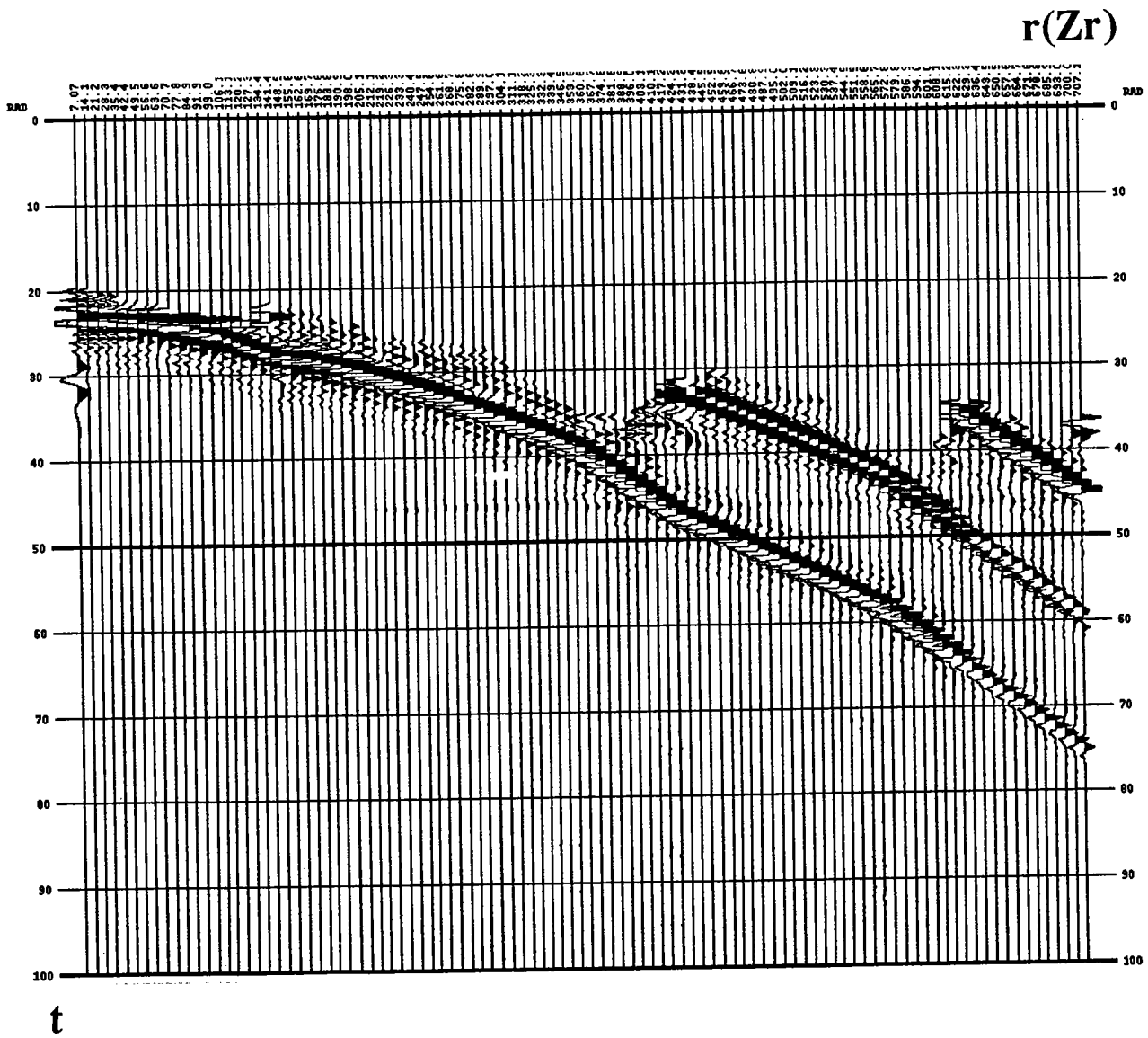

Figure S9. CLP gather for variable slowness medium.

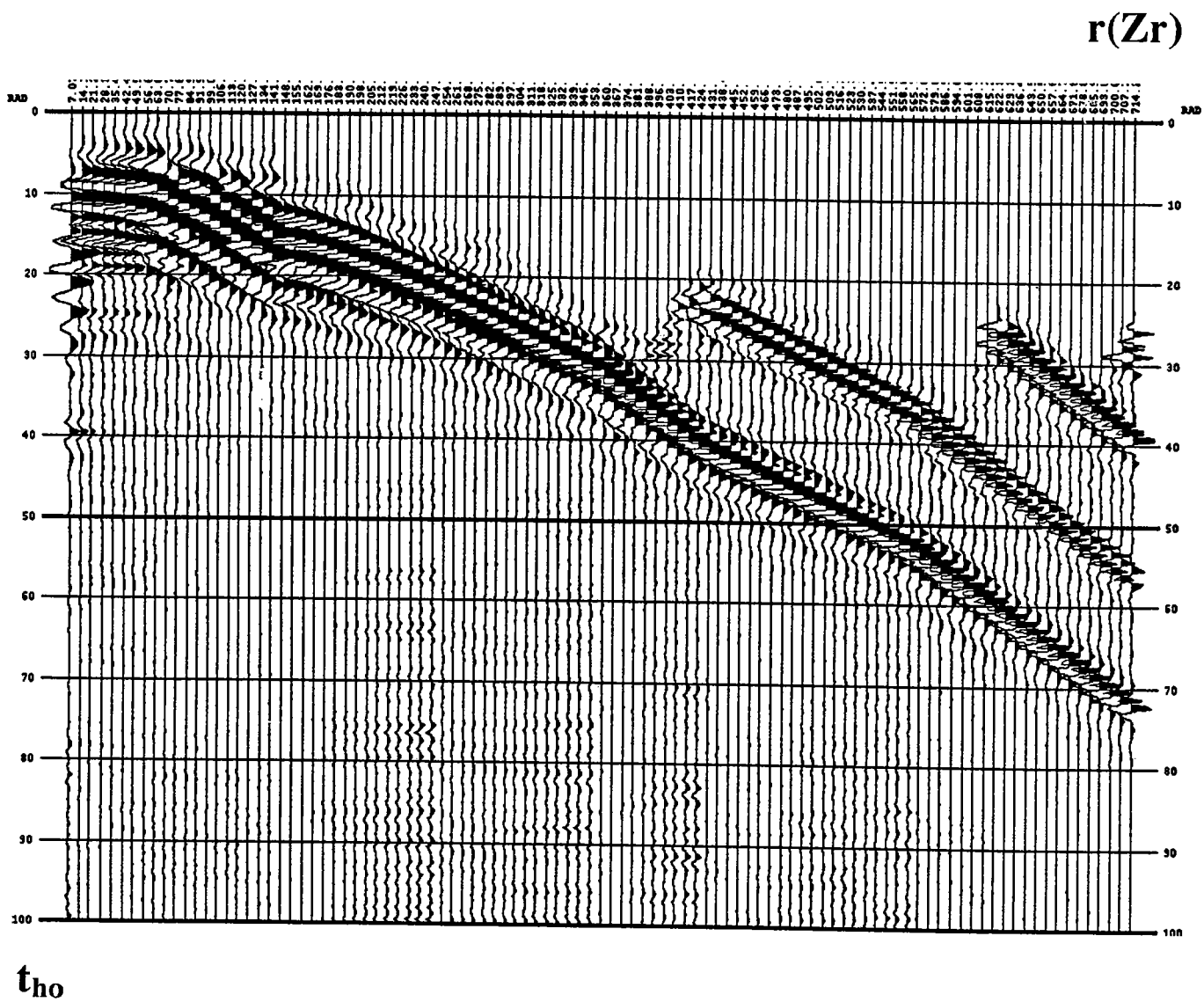

Figure S10. CLP -HNMO gather for variable slowness medium after a constant HNMO slowness has been applied.

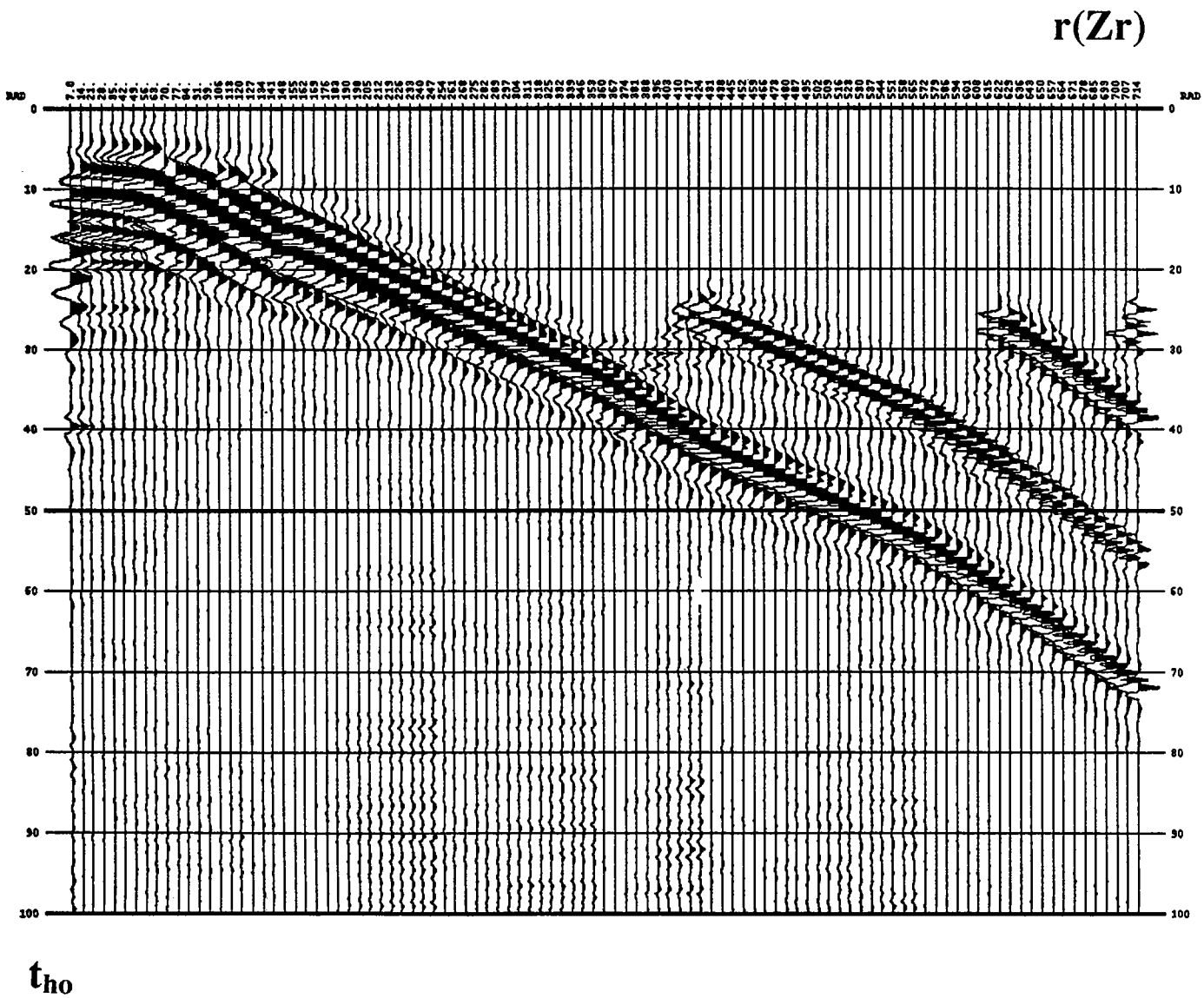

Figure S11. CLP - HNMO gather for variable slowness medium after HNMO residual RMS velocities have been applied for all radial distances.

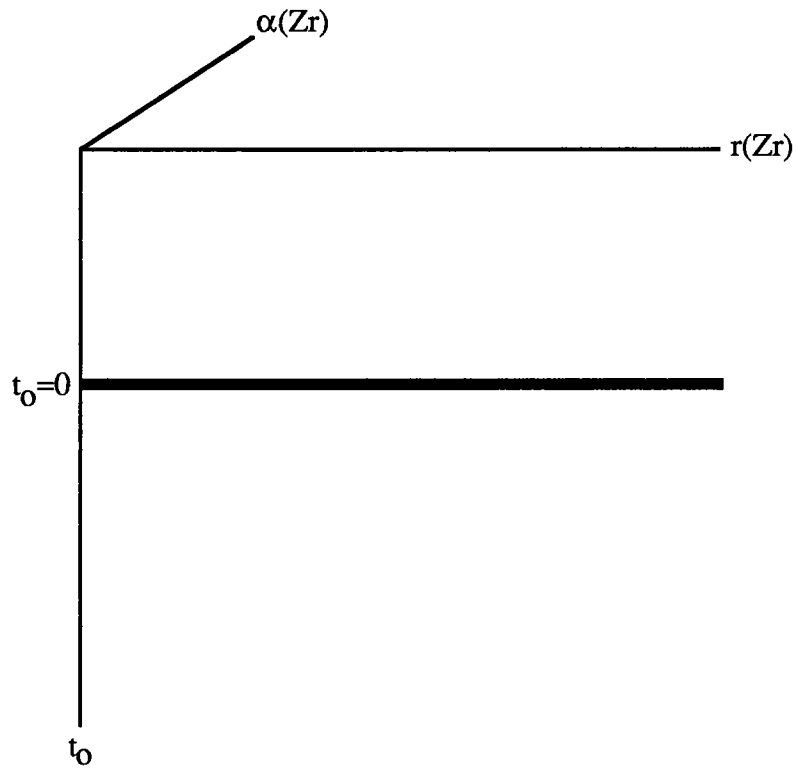

Figure 14. CLP - VLMO gather for variable slowness media.

Synthetic Example

A synthetic example for the variable VLMO velocity is shown for the same synthetic data set as the variable velocity HNMO synthetic example. These CLP-VLMO gathers come after the CLP - HNMO gathers on an incremental radial distance basis. A CLP - VLMO gather for the midpoint between the wells is shown in figure S12 after a single VLMO slowness has been applied. The CLP - VLMO gather after the full sequence of residual VLMO slownesses have been applied is shown in figure S13.

REAL DATA EXAMPLES

The proceeding theory was applied to a West Texas data site. In the following discussion we will discuss two reflections which were imaged by stacking using the preceding theory on cross-well reflection velocity analysis. Figure R1 shows the result of a stack using the above theory. It is one of the strongest reflections in this data set, and was obtained by using cross-well reflection velocity analysis for one lateral point. Downgoing data were

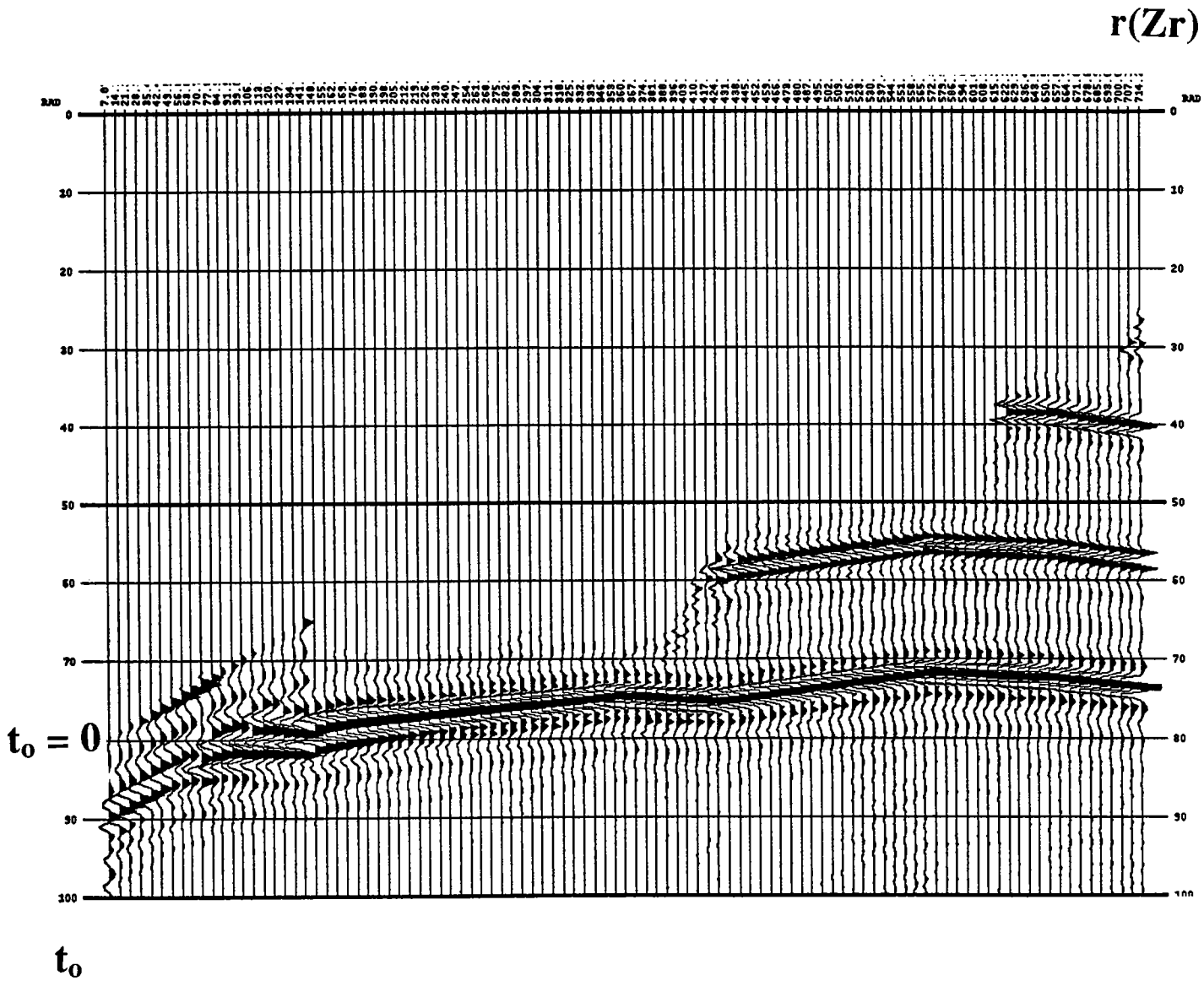

Figure S12. CLP -VLMO gather for variable slowness medium after a constant VLMO slowness has been applied.

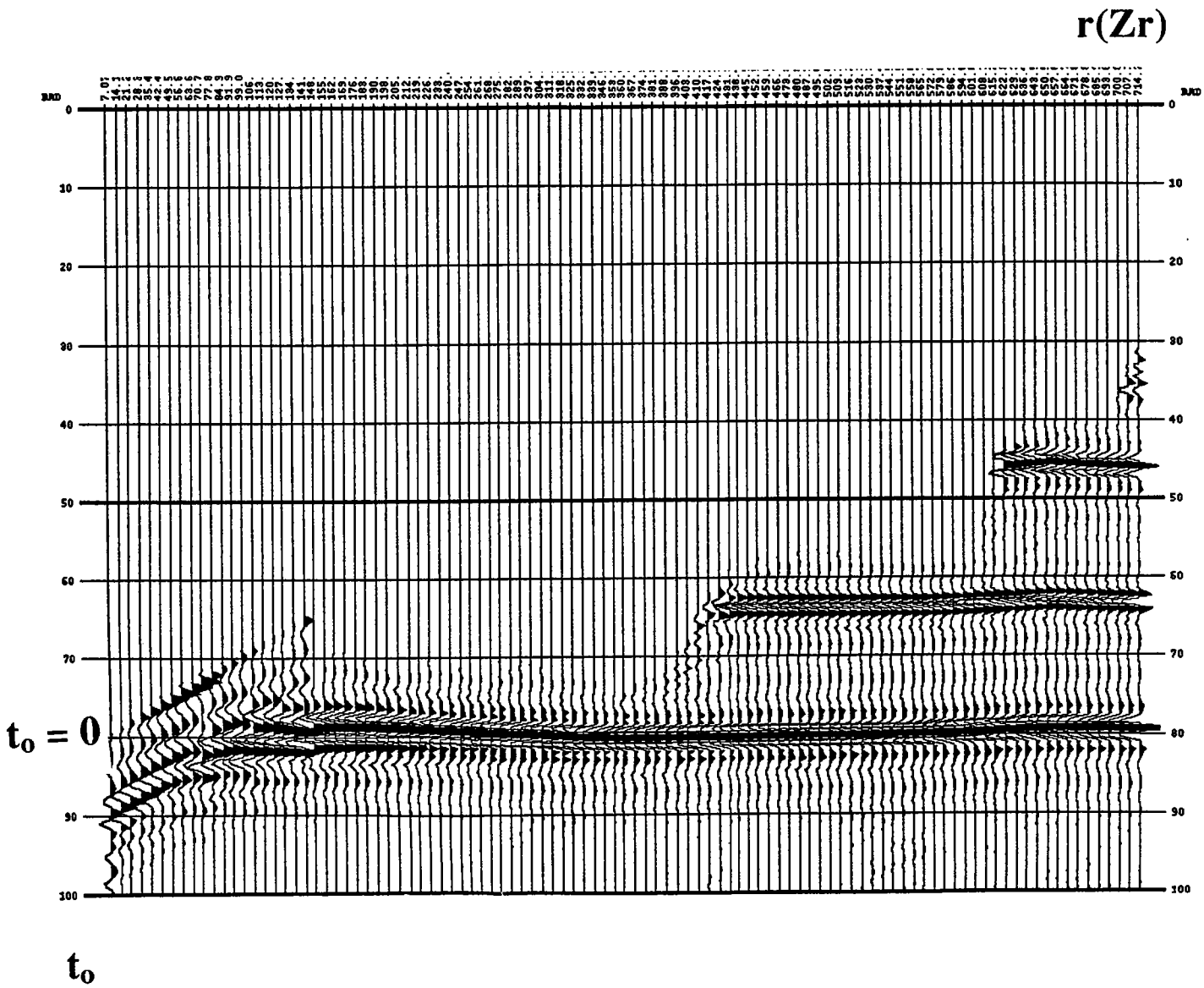

Figure S13. CLP - VLMO gather for variable slowness medium after VLMO residual slownesses have been applied for all radial distances.

used to obtain this stack, so the second reflection below the depth 2850 feet is actually higher in the region with respect to depth. A constant slowness estimated from the tomogram gives the stack shown in figure R2. We see that the stack in figure R1 gives a reflection that is more coherent and has a more accurate depth conversion.

Now we will discuss a more detailed analysis for a reflection that is below this strong reflection. Polar coordinates are calculated for two assumed reflector depths; 2865 feet and 2870 feet. A CLP gather for a lateral point midway between the wells is shown in figure R3 for an assumed reflector depth of 2865 feet. The analysis starts by using the theory outlined in the constant slowness CLP - HNMO section. We want to use a constant slowness HNMO correction to find the correct reflector depth. Through the analysis it was found that the reflection depth of 2865 feet with an HNMO slowness of 1/17.1 ms/ft gave the desired moveout in the CLP - HNMO gather (Figure R4). The data were filtered with a bandpass due to the stretching associated with the HNMO correction. The stretch is the strongest at small radial distances, which correspond to wide angles of incidence. The bandpass was a trapezoid of 300-400-2000-2200 Hz. Shown in figures R5 and R6 are reflection depths and constant slowness HNMO corrections that gave reasonable moveouts but were not used. In figure R7, the slowness that is used allowed the reflection at 2850 feet to intersect the origin. We know it is not at the assumed reflector depth due to its hyperbolic moveout. In figure R8 an apparent event lines up at the origin with a fairly linear moveout. Due to the weakness of the event, along with the inability to track the event through a large range of radial distances, this was dismissed as a side lobe due to the bandpass filter. In figure R9 there is a CLP-HNMO gather that uses a slowness of 1/19 ms/ft. Even though the slowness is too small, we can see the event that we are considering is still quite strong. In figure R10 we consider the same gather with the same HNMO slowness applied, but no longer bandpass filter the data. We can still see the event, and for some radial distances it is stronger than the prominent reflection at 2850 feet (in time). This indicates that this event is a reflection and not a side lobe of the more prominent reflection. We now have to consider variable slowness (velocity) HNMO and VLMO corrections to align the data. We apply both corrections using the theory in the variable velocity section, but we only use the CLP - VLMO gather to align the reflection since we know the event has to be flat in this domain (Figure 14). Figure R11 shows the CLP - VLMO gather (using the lateral point of the midpoint between the wells or $\alpha=\pi/4$) before alignment (after only the previously determined HNMO slowness of 1/17.1 ms/ft, and use of the same slowness for the VLMO correction). Figure R12 shows the CLP - VLMO gather after alignment. Figure R13 shows the resulting stack across the radial distances of 65-115 feet. We see

that we get a coherent stack for many of the lateral points, particularly midway between the wells. To get a reflection that goes all the way across, we need to do velocity analysis for other lateral points. We still use the CLP-HNMO gather to see if there is a reflection at the depth of 2865 ft. for these other lateral points. Figure R14 shows the alignment of the reflection event for a lateral point 1/3 of the distance from the source well. Figure R15 shows the resulting stack. It gives a very coherent reflection for lateral points near 1/3 of the distance from the source-well. Figure R16 shows the alignment of the reflection event for a point 1/5 of the distance from the sources well. Due to the pre-processing some of the reflection was removed. Therefore only small radial distances are used in the stack, and the frequency content is lower. A receiver gather will also have to be used to overcome this problem; only source gathers was used for this analysis. Figure R17 shows the resultant stack. We then combine these three results to give a composite stack for the reflection at 2865 feet. The details for lateral velocity interpolation are still being developed. To give more continuity to the composite stack, a trace mix window of (1,2,1) is applied. This composite is shown in figure R18. The only part of the section that has relevance is at the assumed reflector depth. All of the other amplitude information is ignored. This is compared to the stack using a constant slowness from the tomogram in figure R19. We can see that the reflection is flatter, more coherent, has more lateral points imaged, and has a more accurate depth conversion.

CONCLUSIONS AND FUTURE WORK

In this paper we have developed an approach to cross-well reflection velocity analysis by using previously derived moveout equations from the cross-well CLP stacking coordinate system and have applied it to synthetic and real data. We have separated the slowness - depth ambiguity by using the moveout of the CLP - HNMO gather, and aligned the reflection data to optimize the stack by using the CLP - VLMO gather. A lot of work remains. Some of the future objectives are

1) Using more of the gathers and improving filters to separate signal from noise and correctly identify events to be aligned and their depths.

2) Align reflection events at higher radial distances (smaller angles of incidence).

3) Develop an accurate interpolation method for stacking slowness at different lateral points for a given reflection depth.

4) Improve the CLP polar coordinate calculations by determining interval slownesses from the stacking slownesses and perform raytracing.

ACKNOWLEDGMENTS

The author thanks Jerry Harris for his support and suggestions, Spyros Lazaratos for helpful conversations, and for his help in setting up the synthetic for the constant slowness case, and Mark Van Schaack for creating the synthetic data used in the variable slowness synthetic gathers.

REFERENCES

Claerbout, J., 1985, Imaging the Earth's Interior.

Lazaratos, S., Rector, J.W., Harris, J.M., and Van Schaack, M., 1991, High Resolution Imaging with Cross-Well Reflection Data: STP vol. 2 Paper A.

Lazaratos, S., Rector, J.W., Harris, J.M., and Van Schaack, M., 1992, High Resolution Imaging Of a West Texas Carbonate Reservior: STP vol. 3 No. 1 Paper E.

Smalley, N., 1992, Cross-well Pre-Stack Partial Migration (Theory): STP vol. 3 No.1, Paper M.

Yilmaz, O., 1987, Seismic Data Processing.

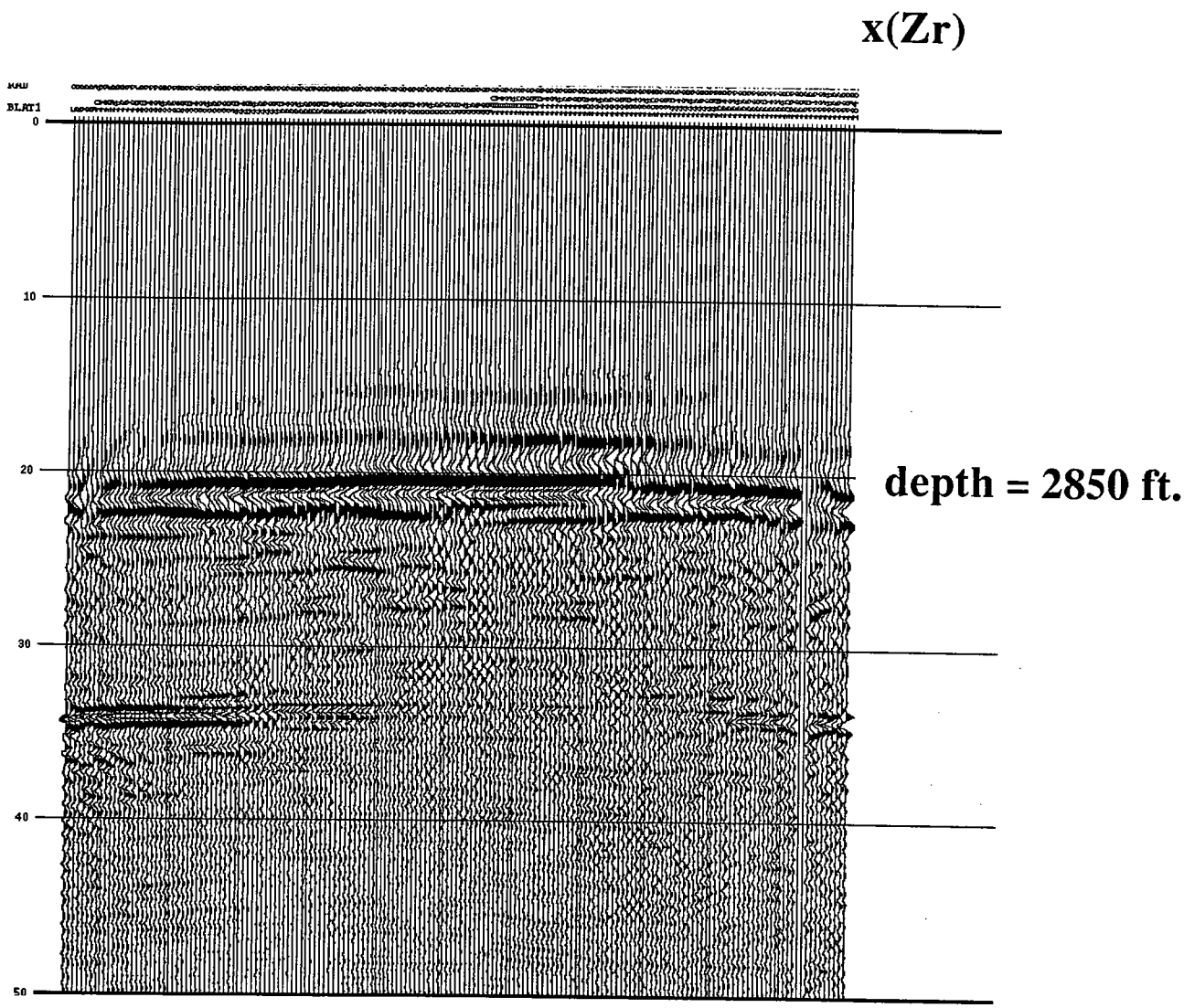

Figure R1. Stacked image of reflection using cross-well velocity analysis theory.

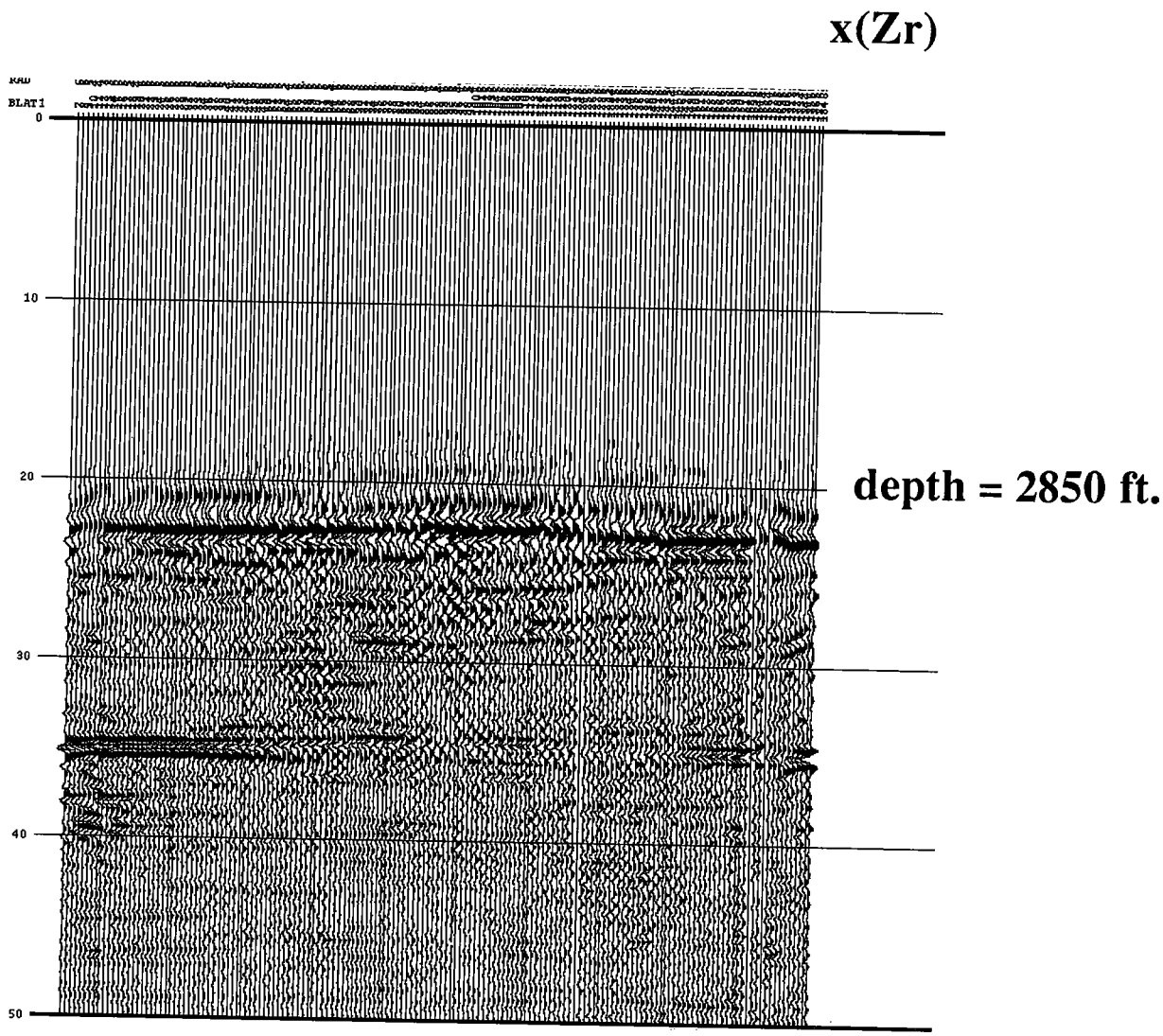

Figure R2. Stacked image of reflection using constant tomogram slowness for HNMO and VLMO corrections.

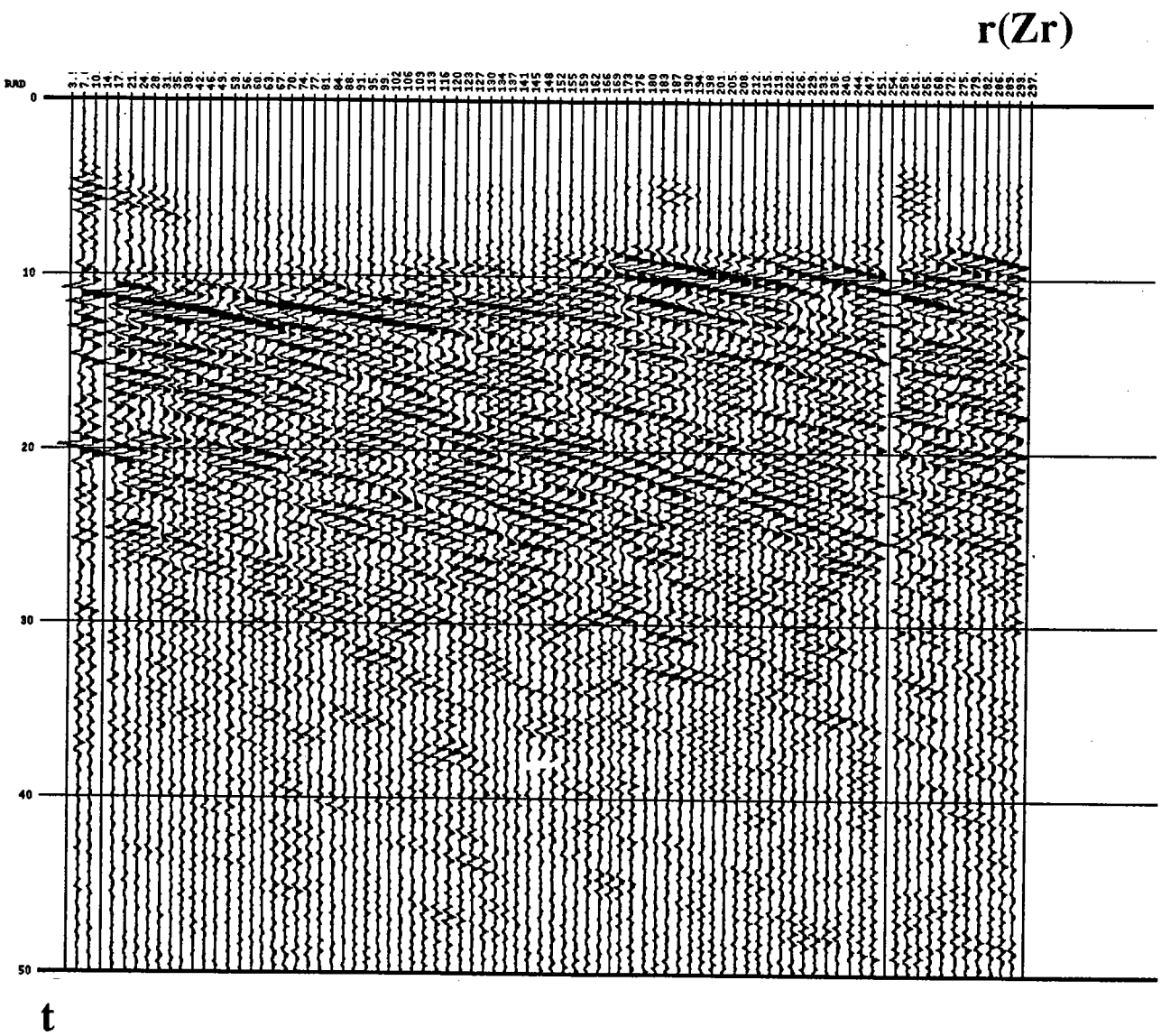

Figure R3. CLP gather for lateral point midway between the wells.

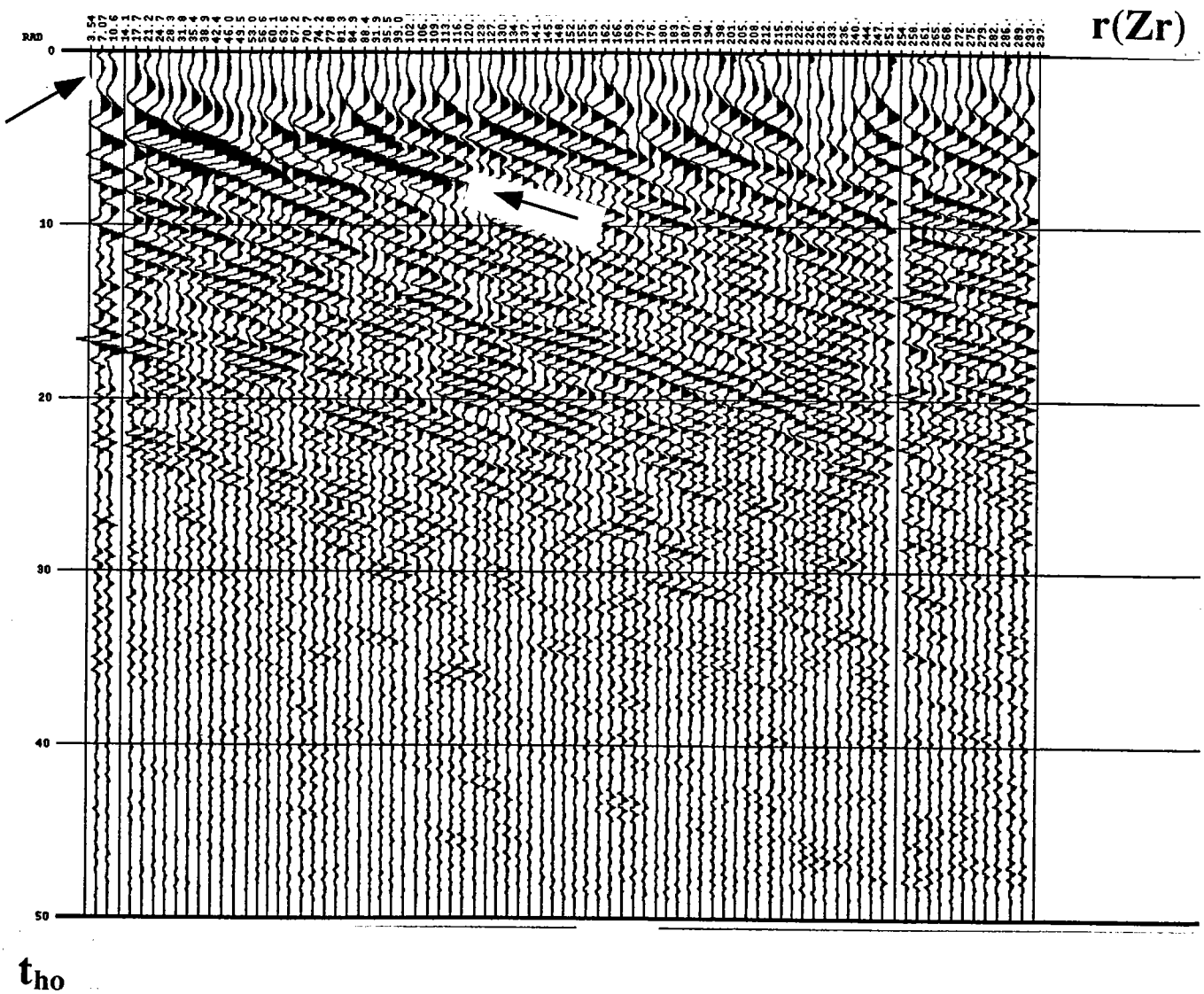

Figure R4. CLP - HNMO gather for reflection depth of 2865 ft and HNMO slowness of 1/17.1 ms/ft. The arrow shows the reflection event.

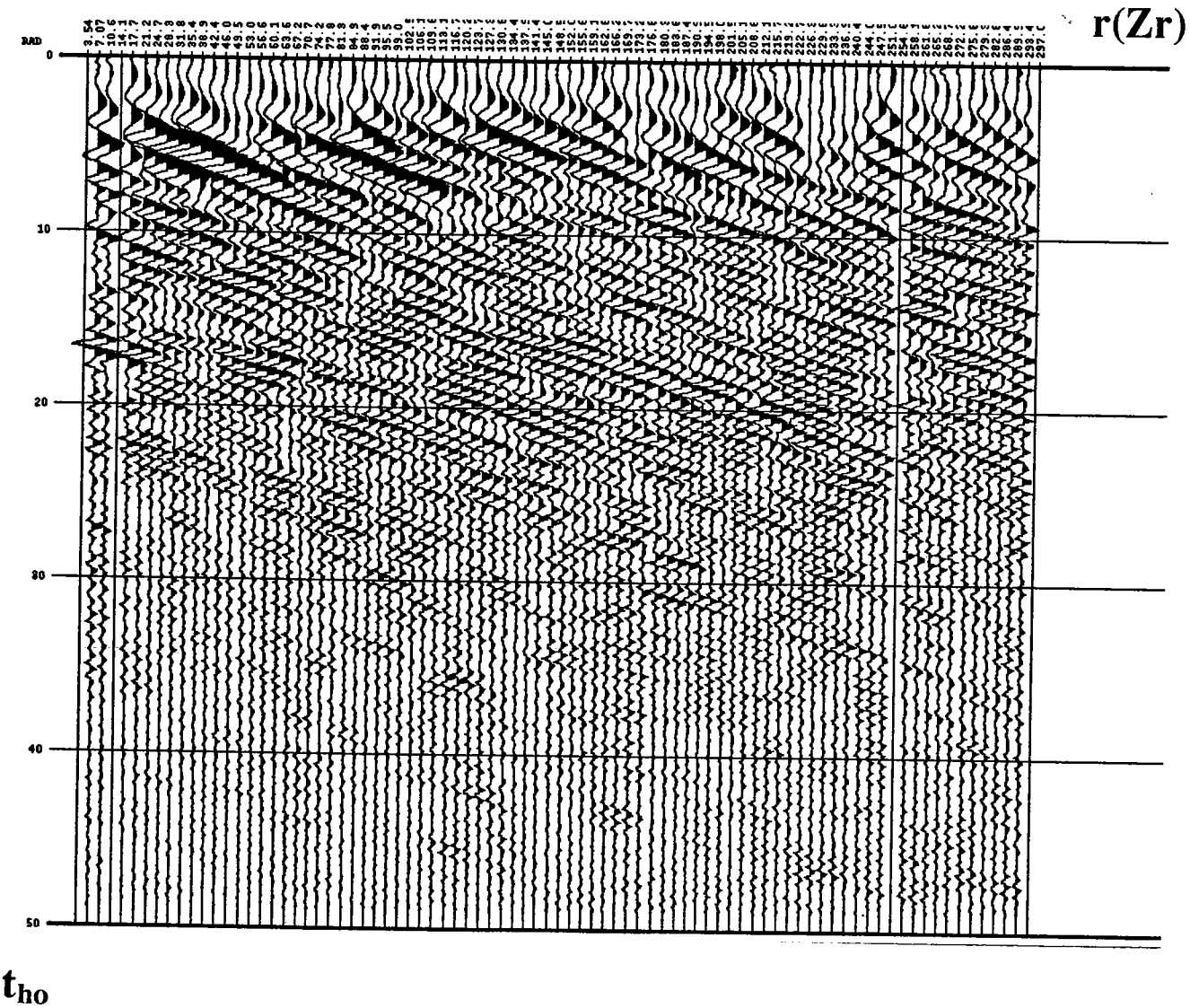

Figure R5. CLP - HNMO gather for reflection depth of 2865 ft and HNMO slowness of 1/16.9 ms/ft.

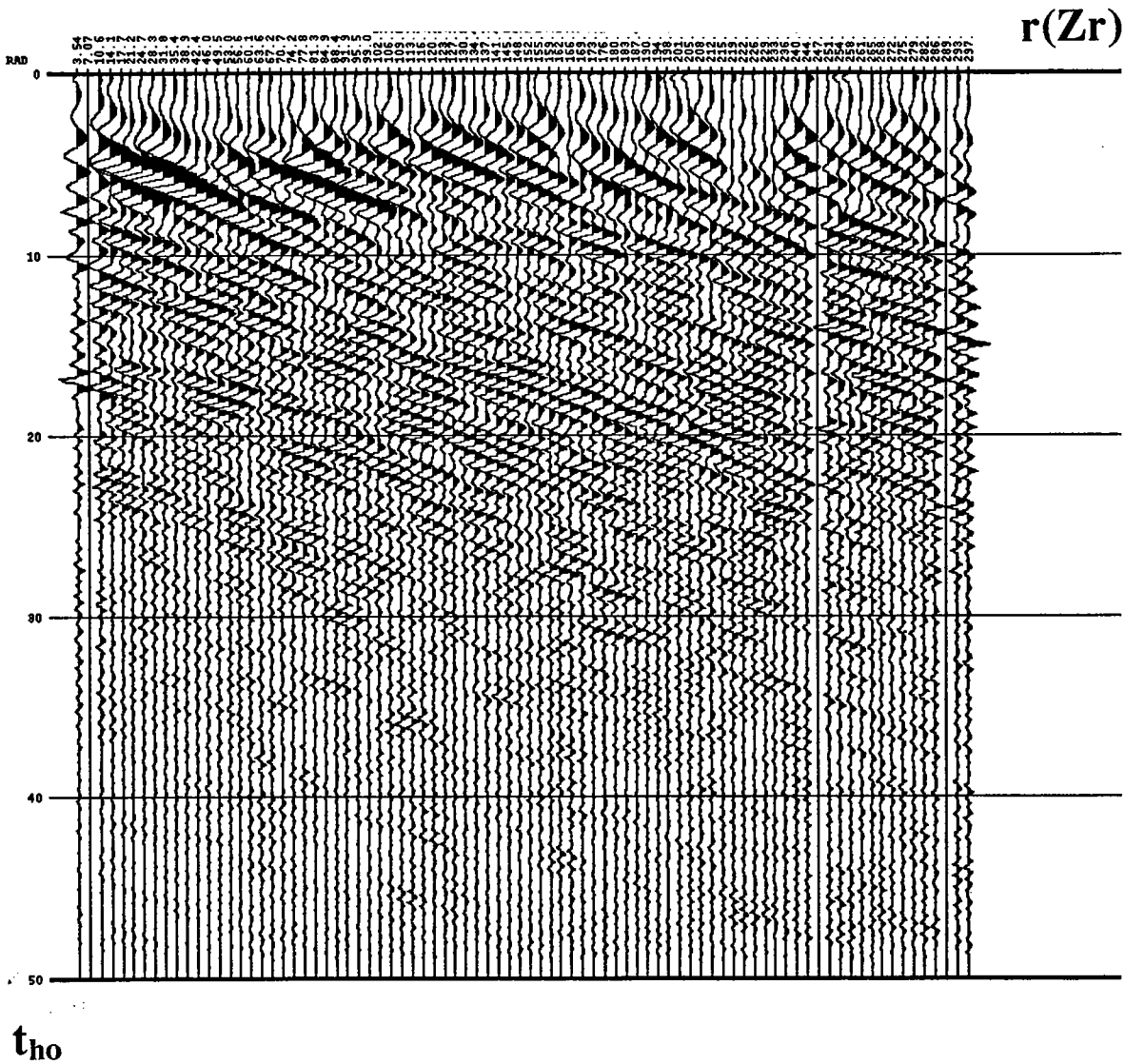

Figure R6. CLP - HNMO gather for reflection depth of 2870 ft and HNMO slowness of 1/17.1 ms/ft.

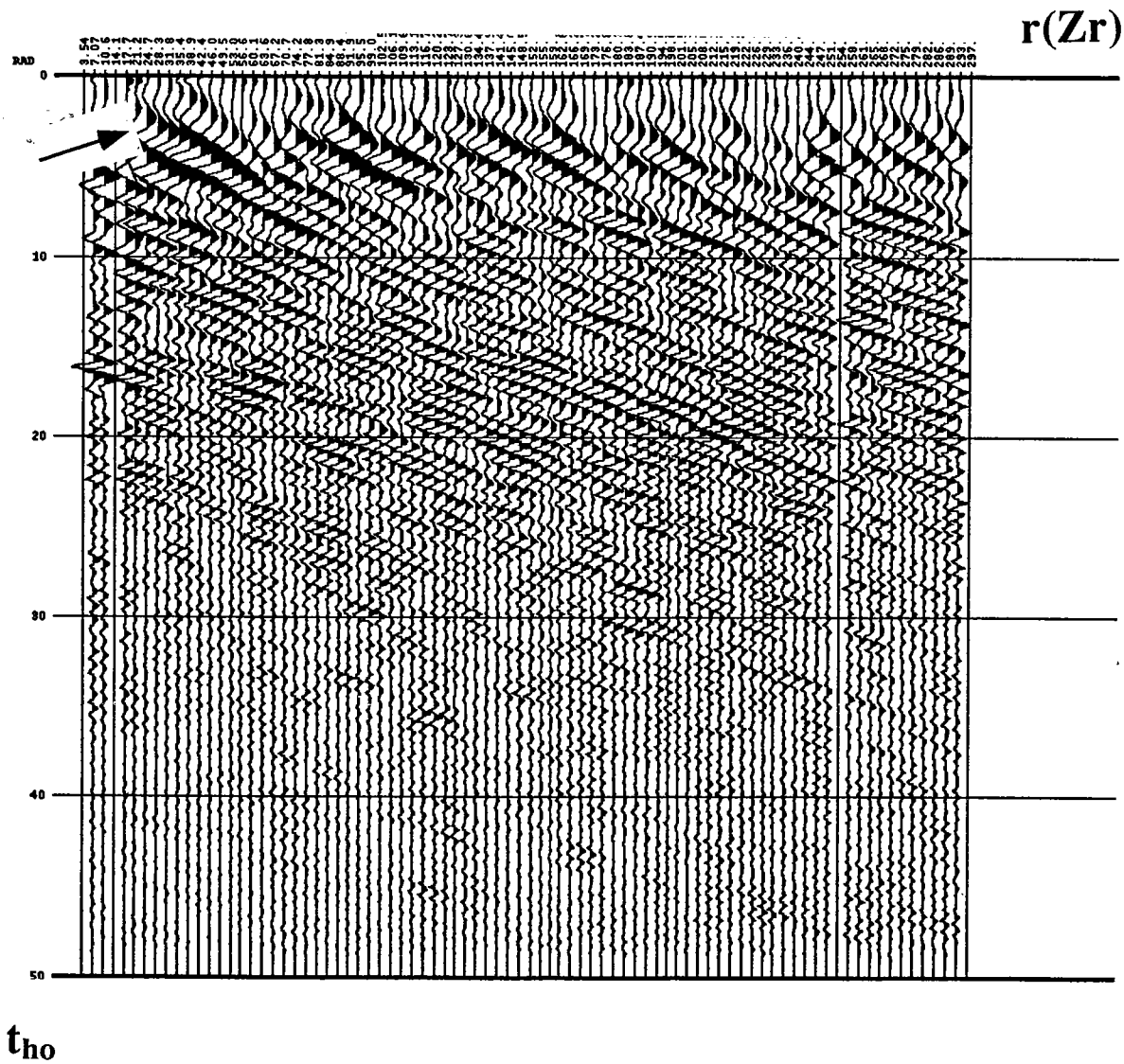

Figure R7. CLP - HNMO gather for reflection depth of 2865 ft and HNMO slowness of 1/16.0 ms/ft. The reflection at 2850 ft approaches the origin with a hyperbolic moveout.

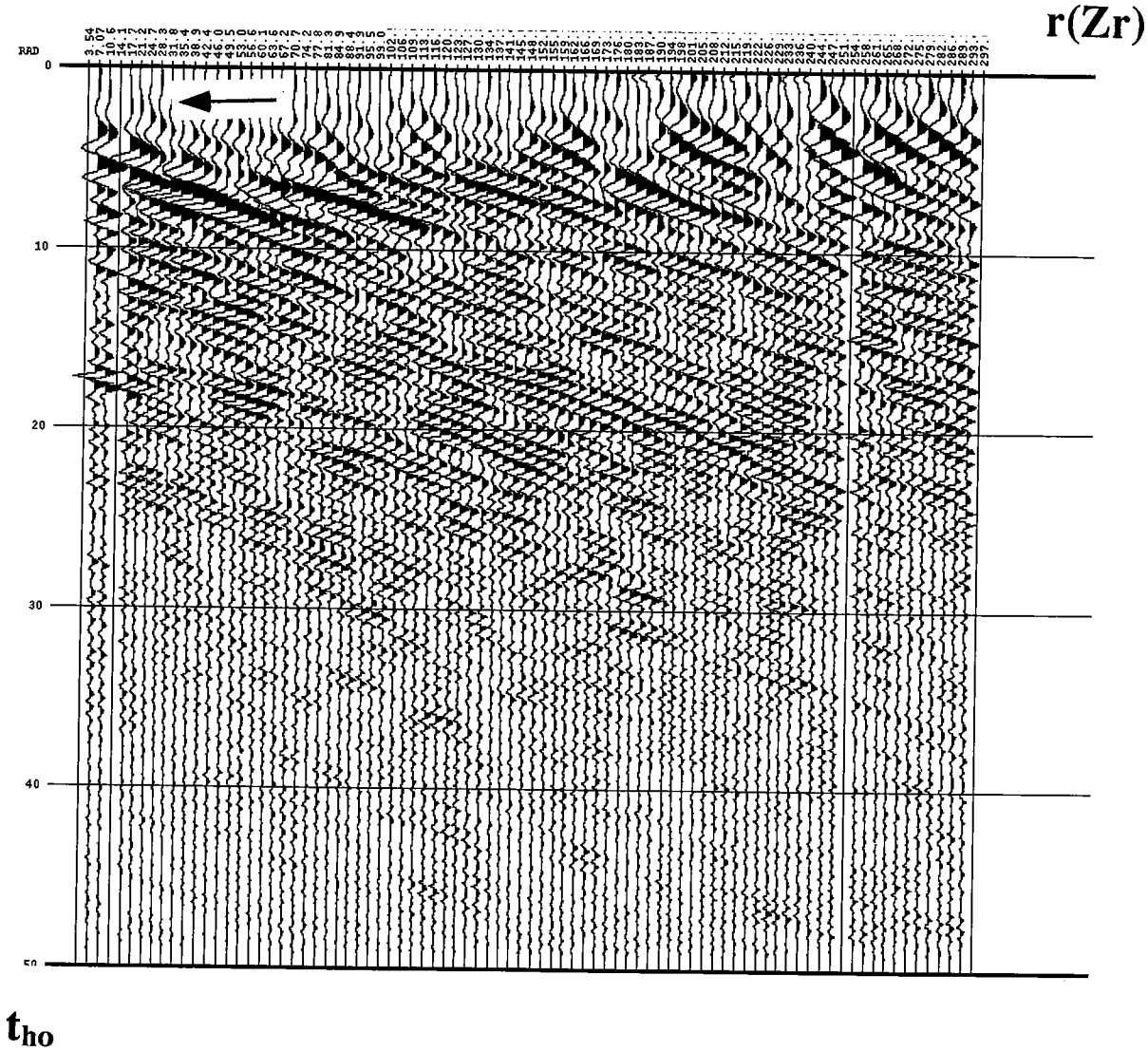

Figure R8. CLP - HNMO gather for reflection depth of 2865 ft and HNMO slowness of 1/18.8 ms/ft. Side lobe of reflection intersects the origin.

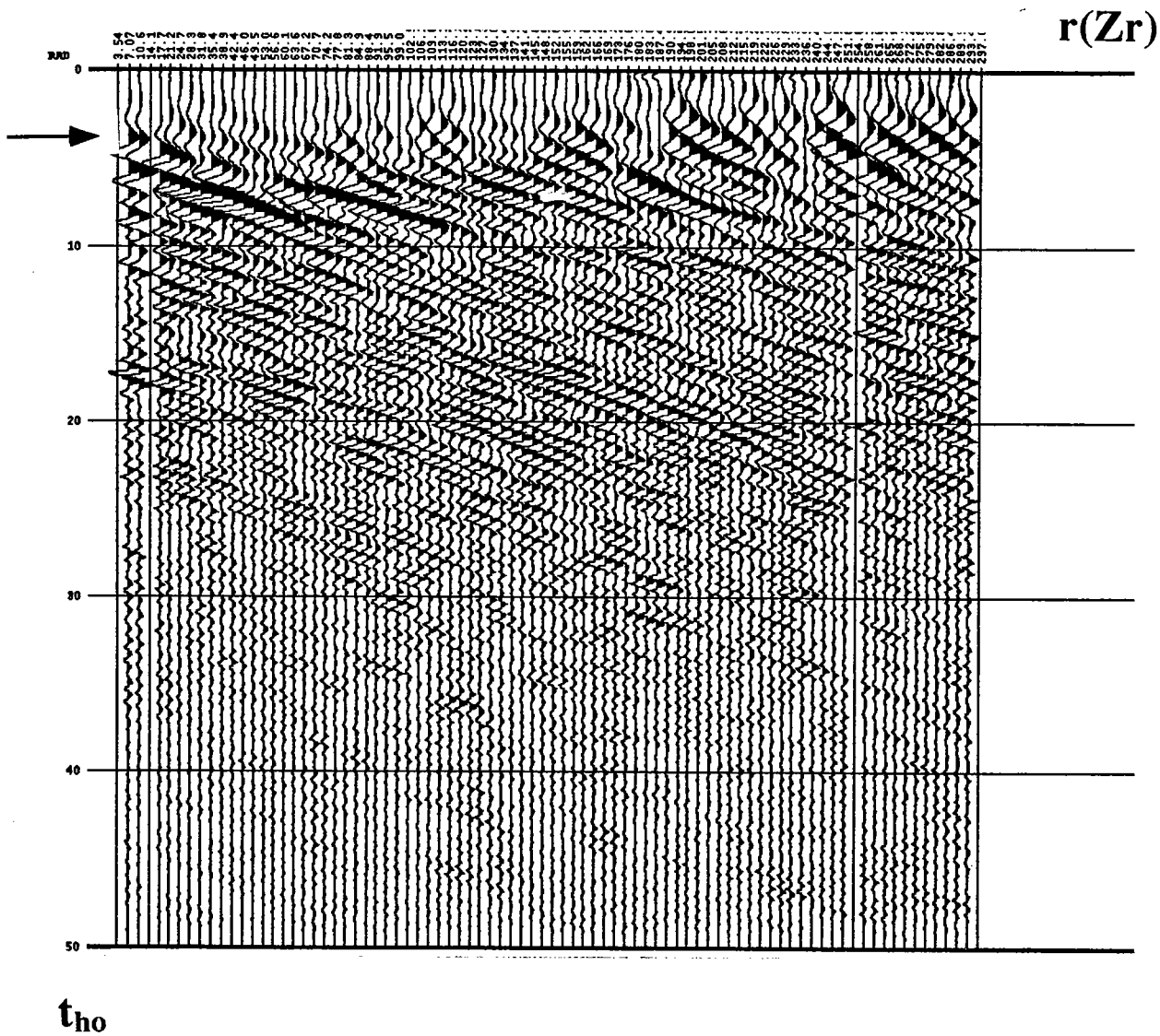

Figure R9. CLP - HNMO gather for reflection depth of 2865 ft and HNMO slowness of 1/19.0 ms/ft.

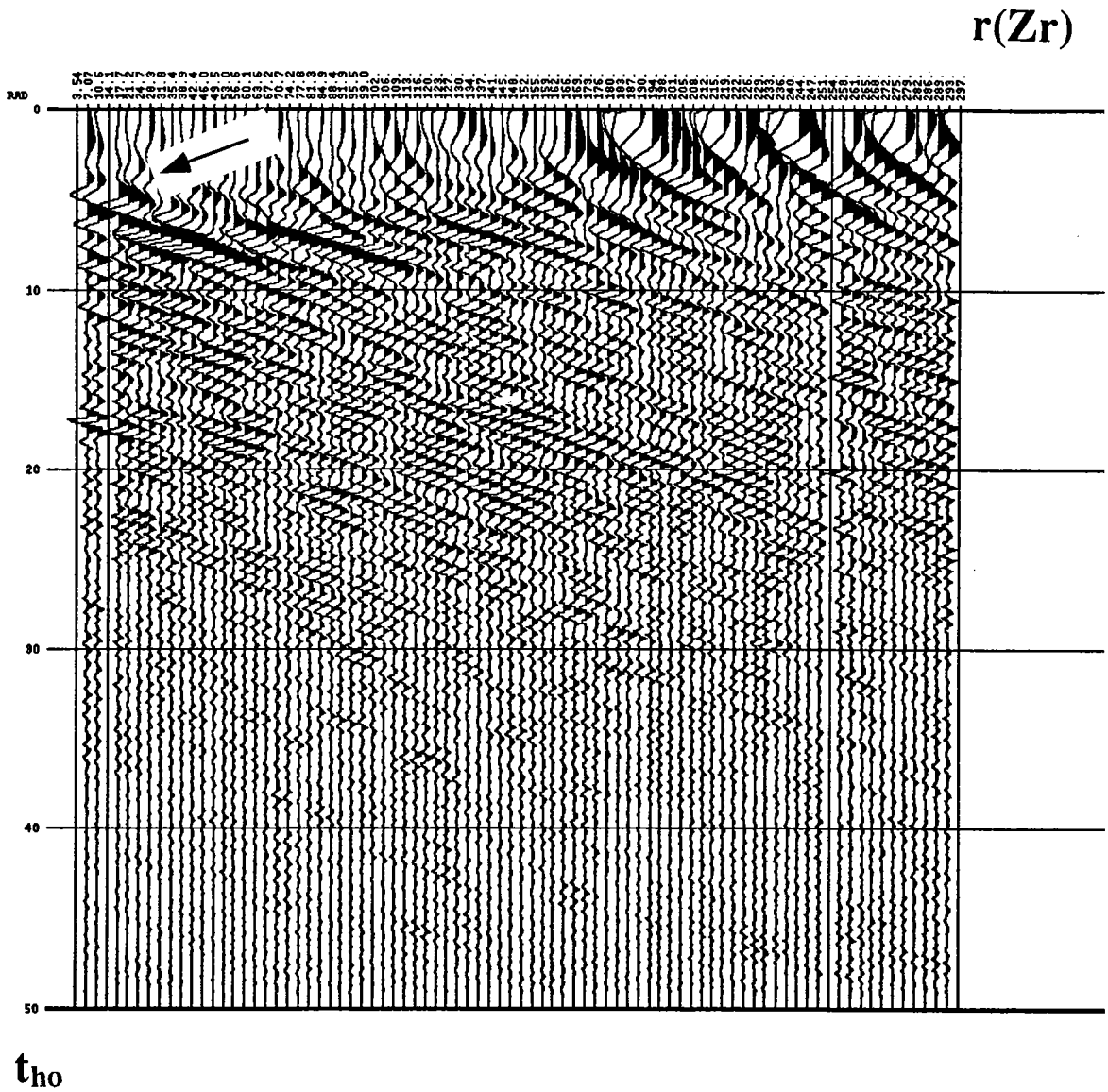

Figure R10. CLP - HNMO gather for reflection depth of 2865 ft and HNMO slowness of 1/19.0 ms/ft. No bandpass filter was applied.

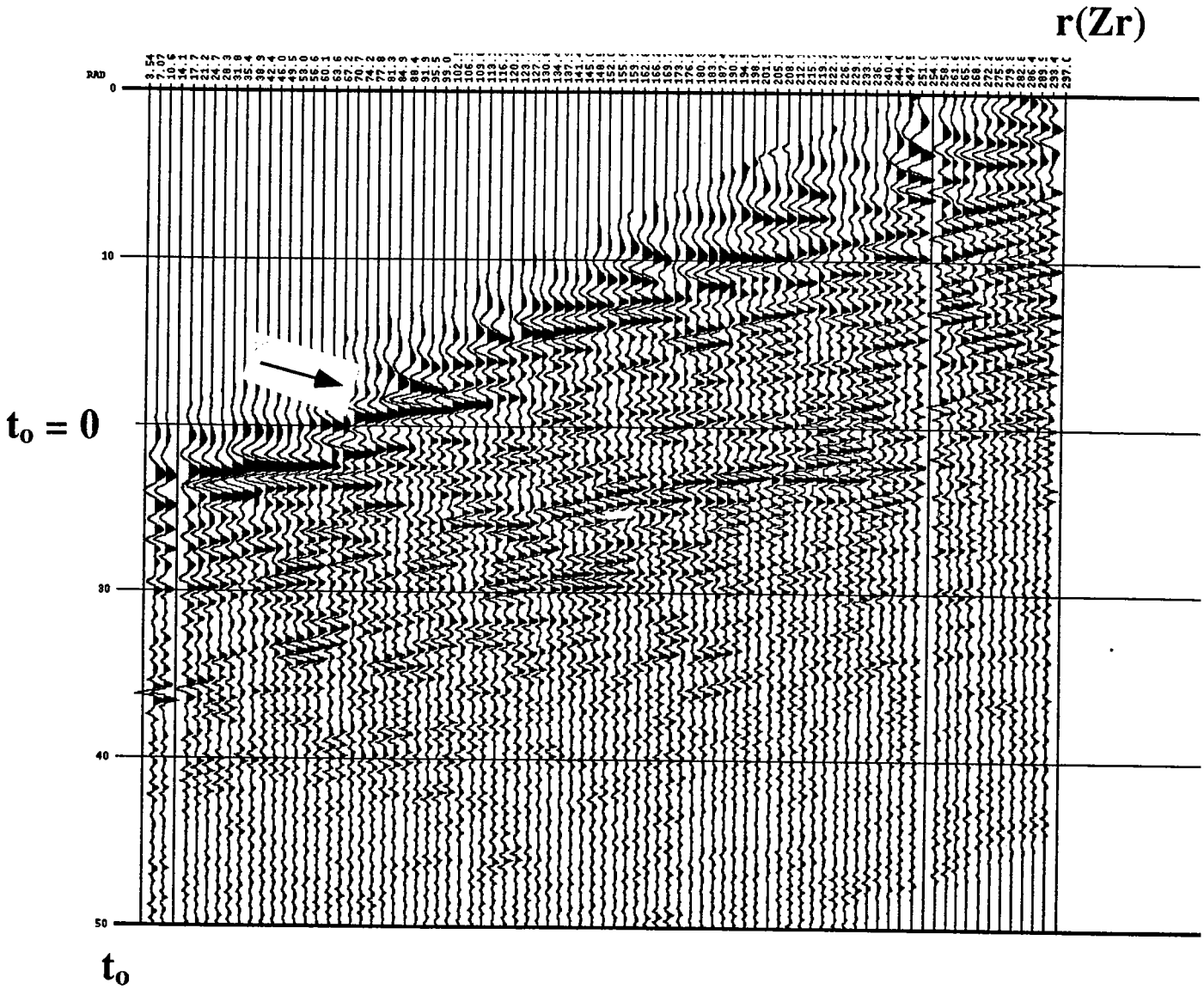

Figure R11. CLP - VLMO gather for reflection depth of 2865 ft after single HNMO and VLMO slownesses have been applied.

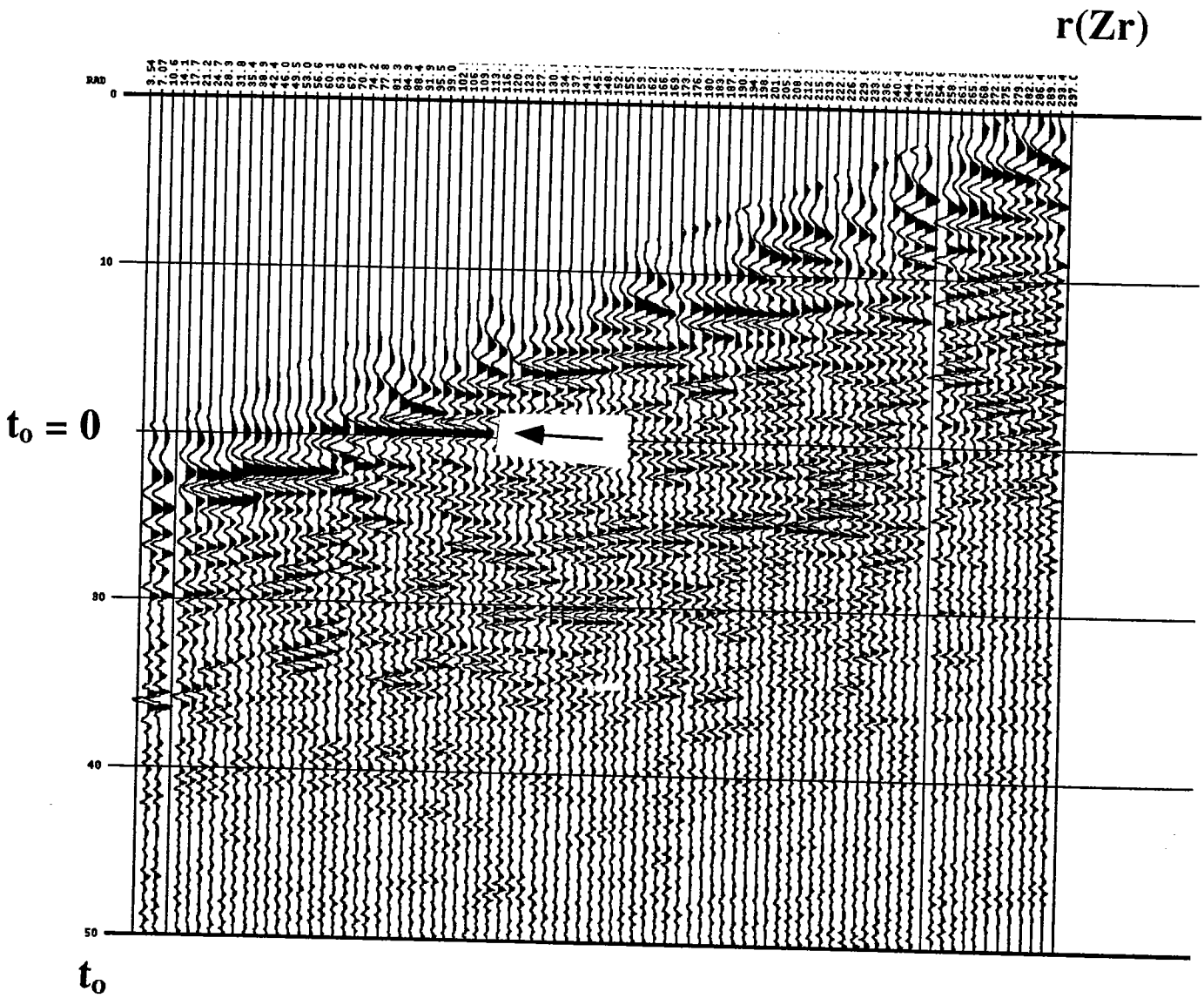

Figure R12. CLP - VLMO gather for reflection depth of 2865 ft after all residual HNMO and VLMO corrections. This is the input to the stack.

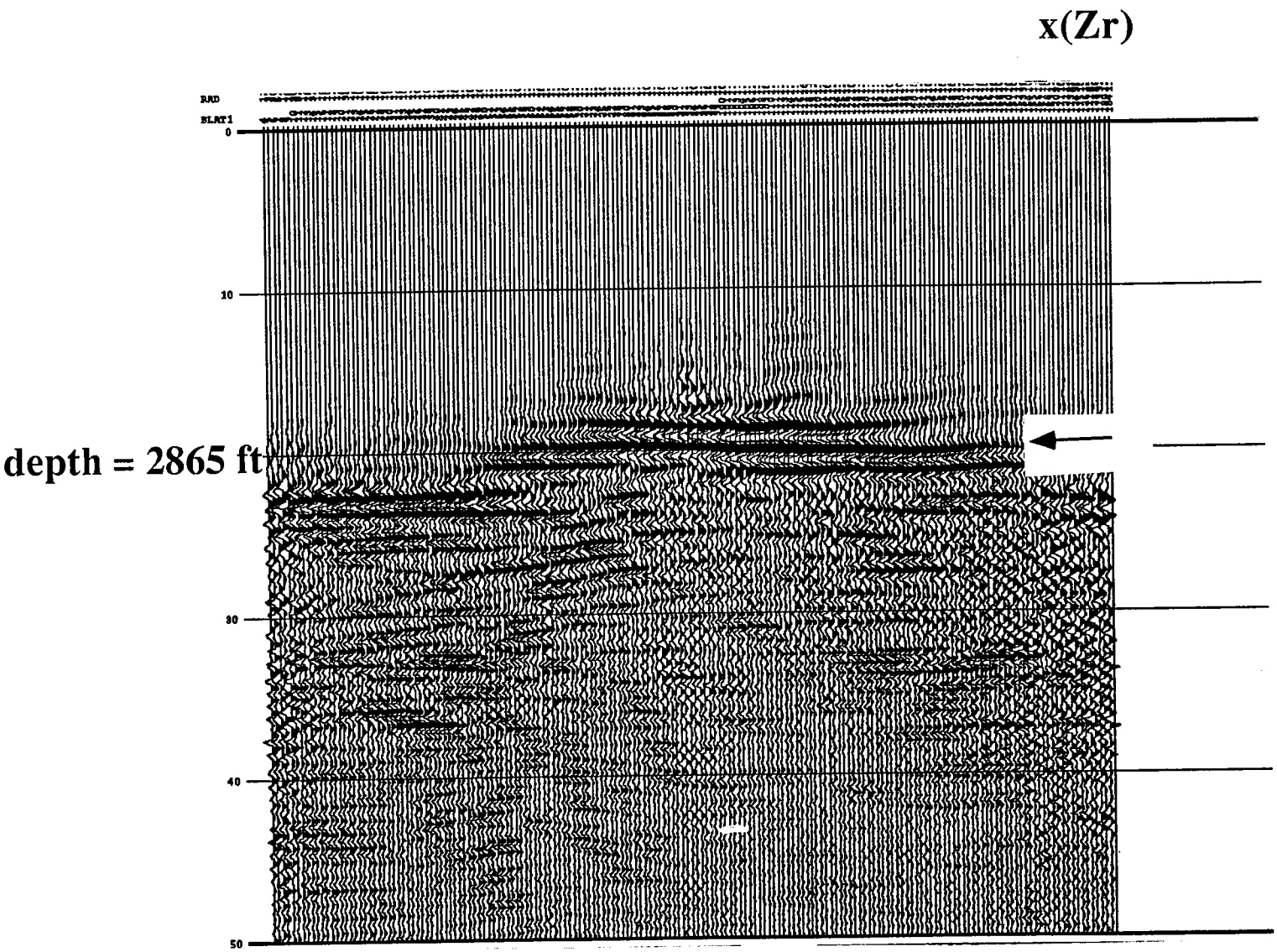

Figure R13. Stack of reflection using HNMO and VLMO residual corrections determined using the CLP gather midway between the wells.

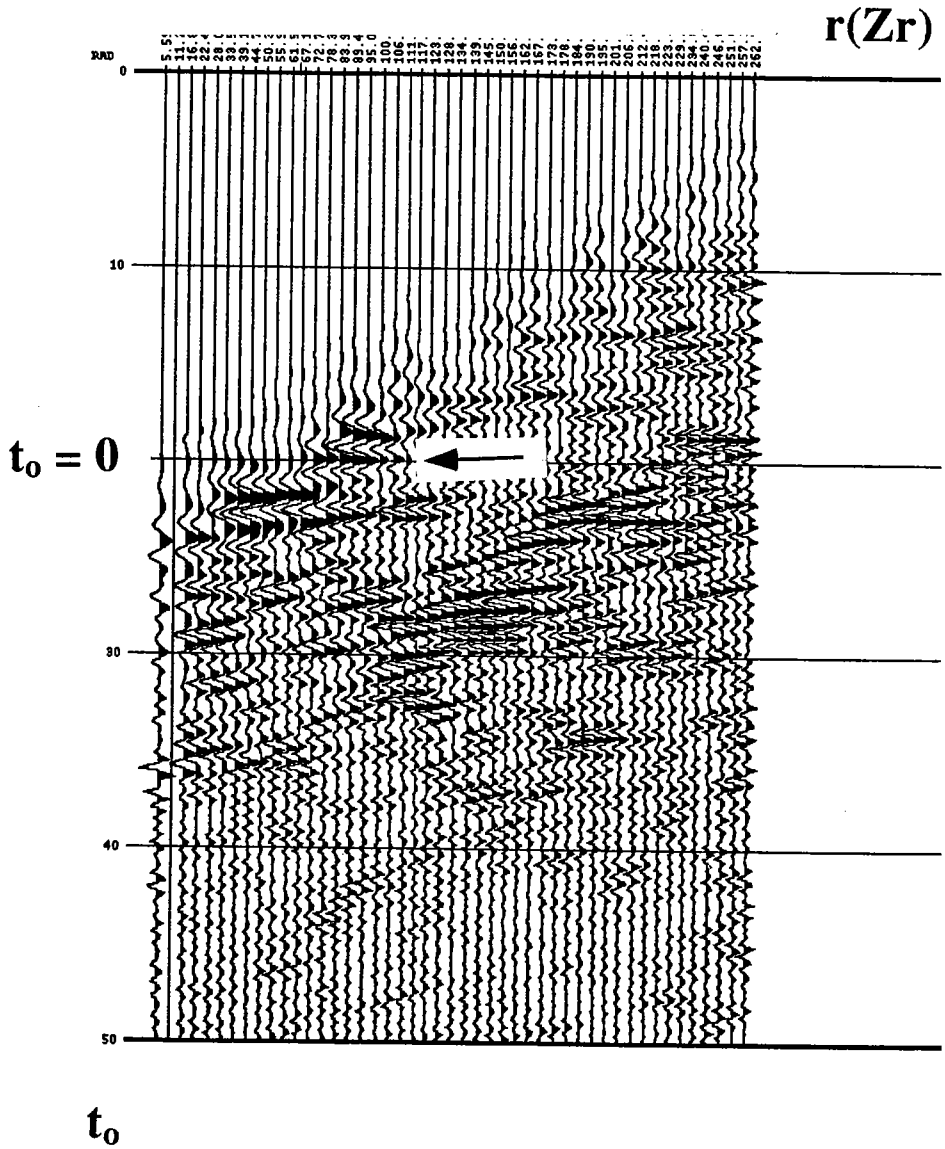

Figure R14. CLP - VLMO gather after HNMO and VLMO residual corrections using CLP gather 1/3 of the distance from the source well.

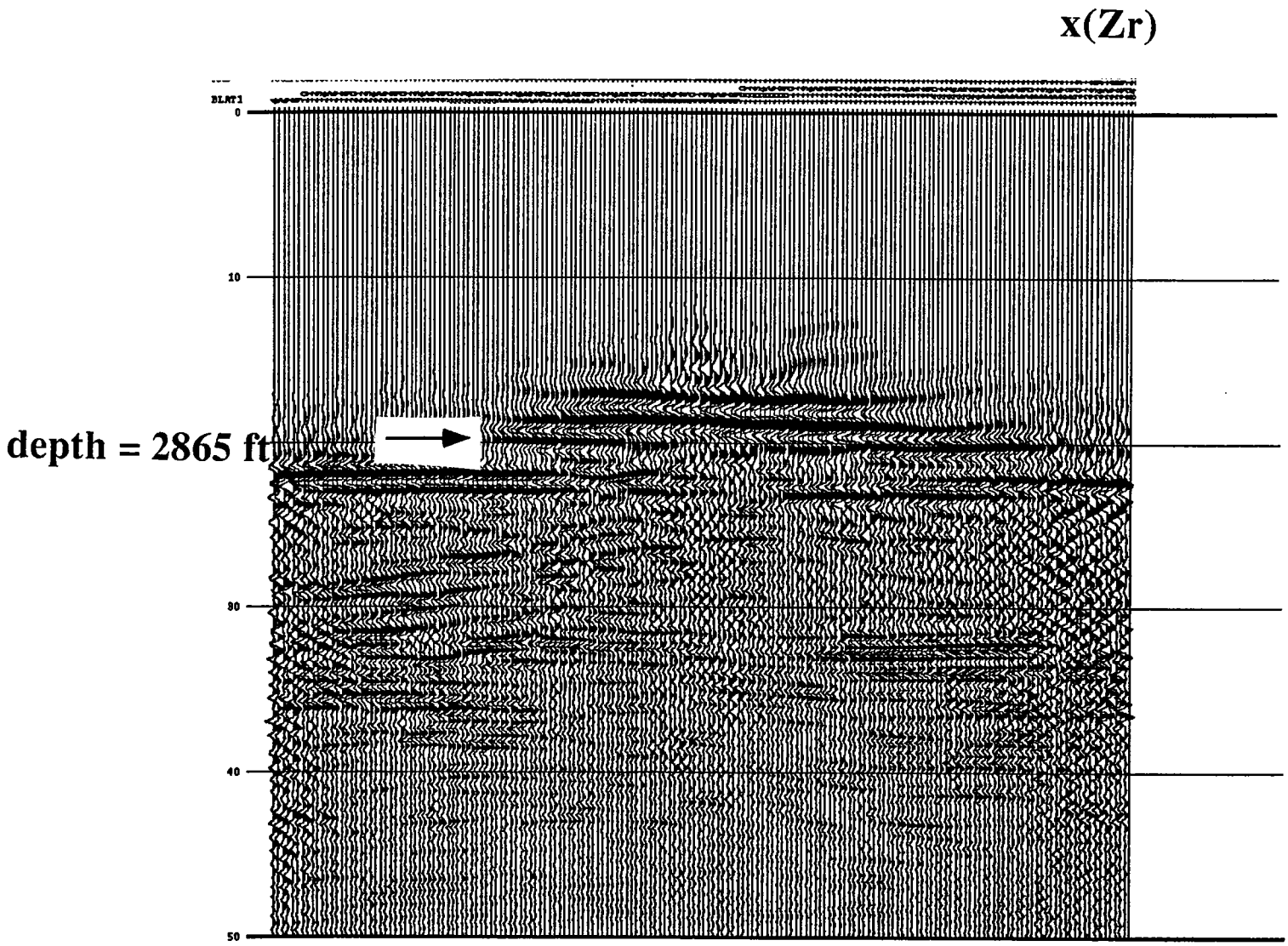

Figure R15. Stack of reflection using HNMO and VLMO residual corrections determined using the CLP gather 1/3 of the distance from the source well.

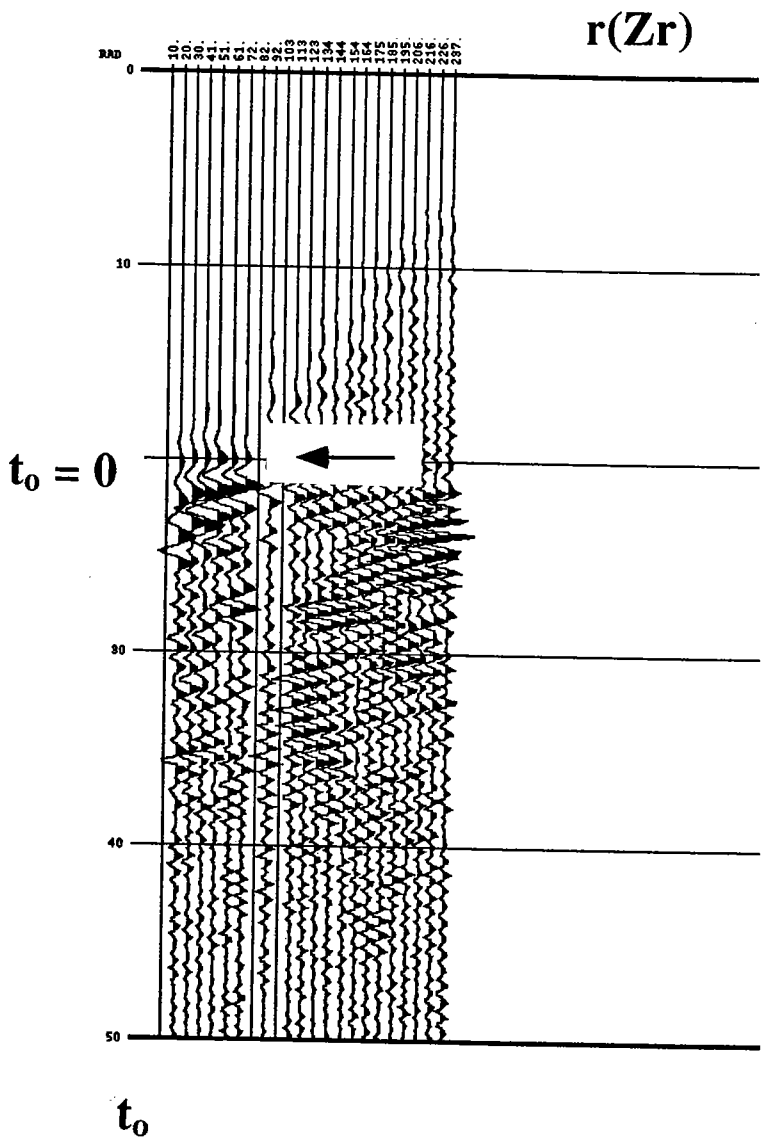

Figure R16. CLP - VLMO gather after HNMO and VLMO residual corrections using CLP gather 1/5 of the distance from the source well.

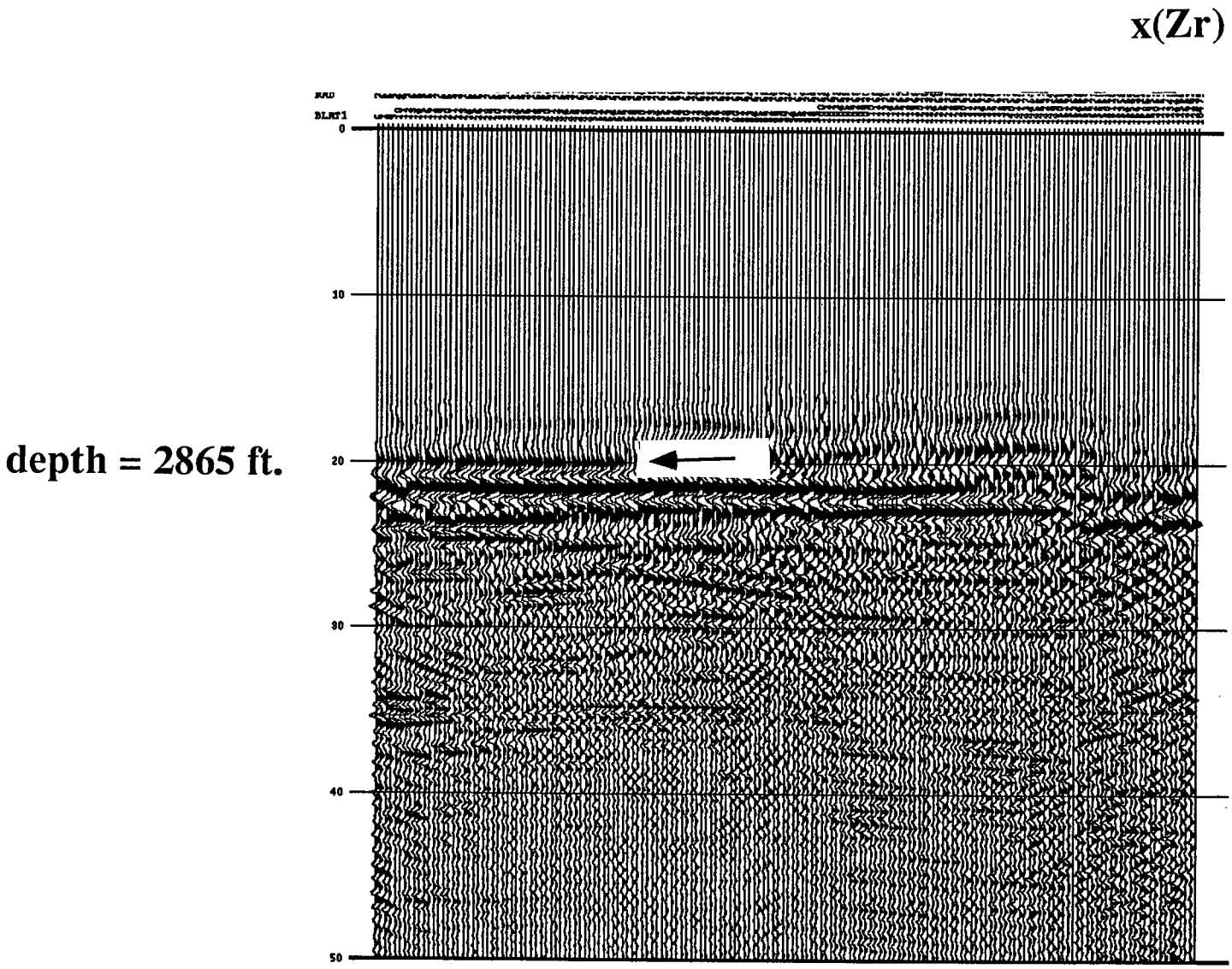

Figure R17. Stack of reflection using HNMO and VLMO residual corrections determined using the CLP gather 1/5 of the distance from the source well.

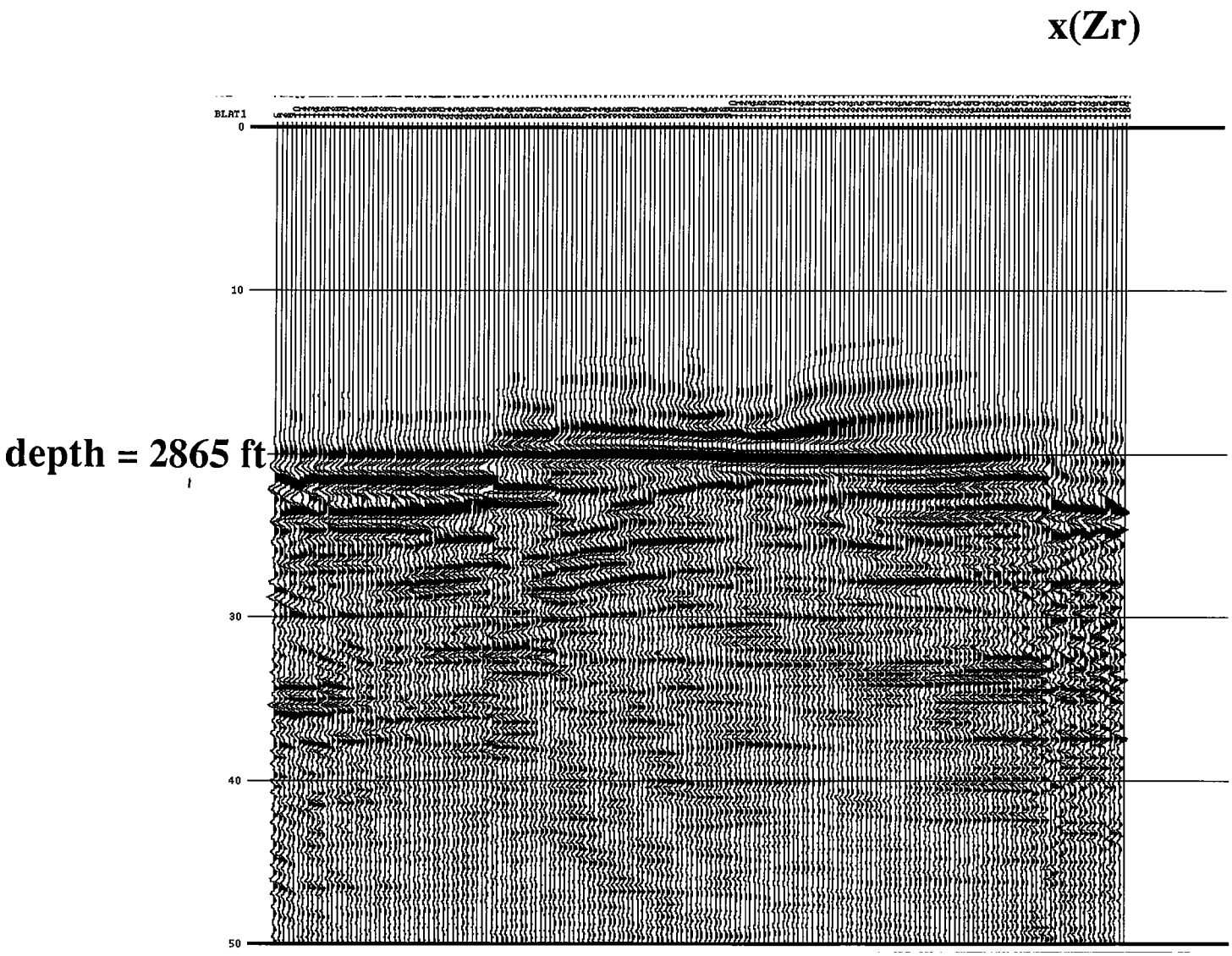

Figure R18. Composite stack.

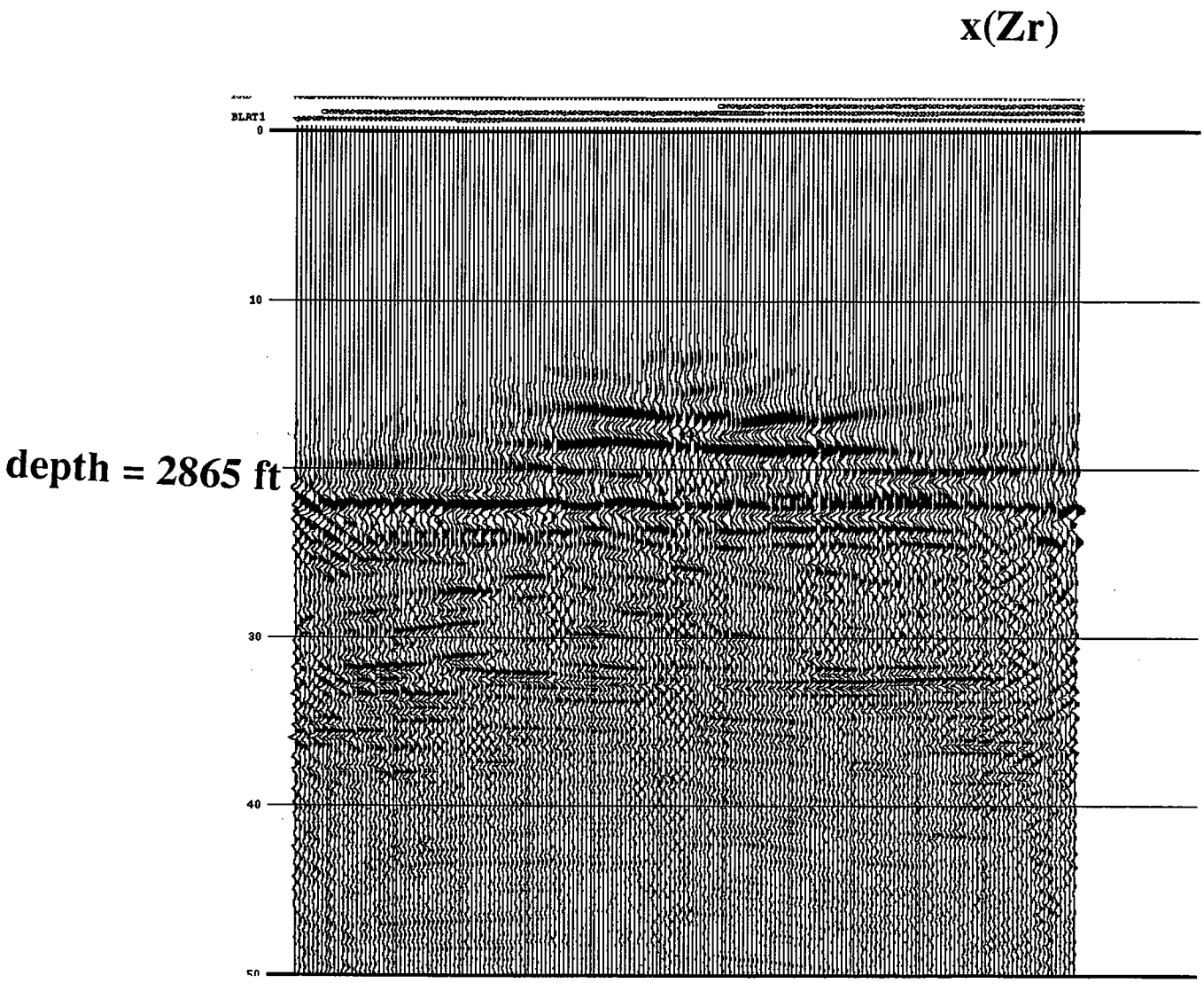

Figure R19. Stack using tomogram slowness for HNMO and VLMO corrections.